

SYKE



NAUTILOS

Deliverable 7.3

Platforms of Opportunity and Ferryboxes
demonstration final report

Date: 30/06/2025

Doc. Version: v3

doi: [10.5281/zenodo.18243335](https://doi.org/10.5281/zenodo.18243335)



Document Control Information

Settings	Value
Deliverable Title	Platforms of Opportunity and Ferryboxes demonstration final report
Work Package Title	WP7 Demonstrations
Deliverable number	D7.3
Description	The report provides a description of the demonstration action technical setup for testing the sensors developed in T3.2, T3.5, T4.1, and T4.4 and integrated in T5.3.2. D7.3. analyses the data collected in relation to other available validation data, assess the TRL levels of sensors, analyse their fit-for-purpose in Platforms of Opportunity for the use in aquaculture and coastal and shelf-sea-related activities and provides recommendations for future developments. SYKE, HCMR, NIVA, DFKI contributed to this deliverable.
Lead Beneficiary	4 - SYKE
Lead Authors	Jukka Seppälä, Sami Kielosto (SYKE), Manolis Ntoumas (HCMR), Sabine Marty, Andrew King, Bert Van Bavel, Øyvind Ødegaard (NIVA), Elmar Berghöfer, Daniel Lukats (DFKI)
Contributors	Sebastian Ehrhart, Noora Haavisto (SYKE), Zacharias Kapelonis, Natalia Stamataki, Manolis Pettas (HCMR), Pierre Jaccard, Elianne Egge, Anette Engesmo, Sonja Kistenich, Louise Valestrand (NIVA)
Submitted by	Jukka Seppälä
Doc. Version (Revision number)	V3
Sensitivity (Security):	Public
Date:	30/06/25

Document Approver(s) and Reviewer(s):

NOTE: All Approvers are required. Records of each approver must be maintained. All Reviewers in the list are considered required unless explicitly listed as Optional.

Name	Role	Action	Date
Gabriele Pieri, Catarina Lemos, Manolis Ntoumas	Review Team 1	<i>Approved high level skeleton draft</i>	18/02/2025
Jana Fahning	Review Team 2	<i>Review finalised</i>	18/06/2025

Document history:

The Document Author is authorized to make the following types of changes to the document without requiring that the document be re-approved:

- Editorial, formatting, and spelling
- Clarification

To request a change to this document, contact the Document Author or Owner.

Changes to this document are summarized in the following table in reverse chronological order (latest version first).

Revision	Date	Created by	Short Description of Changes
V0	29/01/25	M. Martinelli, M. Ntoumas	Preliminary structure
V1	15/06/25	All contributors	Partner's contributions added to draft
V2	16/06/25	Jukka Seppälä	Finalised document, ready for revision from Review Team 2.
V3	30/06/25	All contributors	Final version

Configuration Management: Document Location

The latest version of this controlled document is stored in the project GoogleDrive.

Nature of the deliverable		
R	Report	x
DEC	Websites, patents, filing, etc.	
DEM	Demonstrator	
O	Other	

Dissemination level		
PU	Public	x
CO	Confidential, only for members of the consortium (including the Commission Services)	

ACKNOWLEDGEMENT

This report forms part of the deliverables from the NAUTILOS project which has received funding from the European Union's Horizon 2020 research and innovation programme under grant agreement No 101000825. The Community is not responsible for any use that might be made of the content of this publication.

NAUTILOS - New Approach to Underwater Technologies for Innovative, Low-cost Ocean observation is an H2020 project funded under the Future of Seas and Oceans Flagship Initiative, coordinated by the National Research Council of Italy (CNR, Consiglio Nazionale delle Ricerche). It brings together a group of 21 entities from 11 European countries with multidisciplinary expertise ranging from ocean instrumentation development and integration, ocean sensing and sampling instrumentation, data processing, modelling and control, operational oceanography and biology and ecosystems and biogeochemistry such, water and climate change science, technological marine applications and research infrastructures.

NAUTILOS will fill-in marine observation and modelling gaps for chemical, biological and deep ocean physics variables through the development of a new generation of cost-effective sensors and samplers, the integration of the aforementioned technologies within observing platforms and their deployment in large-scale demonstrations in European seas. The fundamental aim of the project will be to complement and expand current European observation tools and services, to obtain a collection of data at a much higher spatial resolution, temporal regularity and length than currently available at the European scale, and to further enable and democratise the monitoring of the marine environment to both traditional and non-traditional data users.

NAUTILOS is one of two projects included in the EU's efforts to support the European Strategy for Plastics in a Circular Economy by supporting the demonstration of new and innovative technologies to measure the Essential Ocean Variables (EOV).

More information on the project can be found at: <http://nautilus-h2020.eu/>.

COPYRIGHT

© NAUTILOS Consortium. Copies of this publication – also of extracts thereof – may only be made with reference to the publisher.

TABLE OF CONTENTS

ACKNOWLEDGEMENT	5
COPYRIGHT	5
EXECUTIVE SUMMARY	8
LIST OF FIGURES	9
LIST OF TABLES	11
LIST OF ACRONYMS AND ABBREVIATIONS	11
I. INTRODUCTION	13
II. DRONES WITH MULTI- AND HYPER-SPECTRAL CAMERAS AND LIF LIDAR. DEMONSTRATION REPORT (NIVA)	14
1. Background.....	14
2. Demonstration Plan.....	14
Demonstration on UAVs and ASV in the Norwegian Coastal Seas.....	14
3. Results – Comments – Conclusions.....	21
III. IR TEMPERATURE SENSOR DEMONSTRATION REPORT (HCMR)	27
1. Background.....	27
2. Demonstration Plan.....	27
Demonstration on board R/V PHILIA.....	27
3. Results – Comments – Conclusions.....	30
IV. SAMPLER FOR PHYTOPLANKTON AND OTHER SUSPENDED MATTER. DEMONSTRATION REPORT (NIVA)	34
1. Background.....	34
2. Demonstration Plan.....	34
Demonstration on MS Trollfjord Ferrybox.....	34
3. Results – Comments – Conclusions.....	36
V. LOW-COST MICROPLASTIC SENSORS BASED ON SELECTIVE NILE RED STAINING AND FLUORESCENCE DETECTION. DEMONSTRATION REPORT (NIVA)	39
1. Background.....	39
2. Demonstration Plan.....	39
Demonstration of microplastic sampler in M/S Hurtigruten.....	39
3. Results – Comments – Conclusions.....	42
VI. CARBONATE SYSTEM/OCEAN ACIDIFICATION SENSOR. DEMONSTRATION REPORT (SYKE, NIVA)	44
1. Background.....	44
2. Demonstration Plan.....	44

Demonstration on Ferrybox system in Baltic Sea (Syke).....	44
3. Results – Comments – Conclusions.....	48
VII. FERRYBOX STREAM DATA ANALYSIS DEMONSTRATION REPORT (DFKI)	54
1. Background	54
2. Demonstration Plan	54
Demonstration on annotated data from MS Color Fantasy.....	54
3. Results – Comments – Conclusions.....	56
VIII. ETHICAL CONSIDERATIONS	58
1. Data Protection	58
2. Environmental Protection	58
3. Health and Safety	58
4. Protection of Marine Life	58
5. Dual Use Potential.....	58
IX. SUMMARY	59
APPENDIX 1: REFERENCES AND RELATED DOCUMENTS	60

EXECUTIVE SUMMARY

The main objective of Task 7.2 (Demonstration on platforms of opportunity) was to provide field demonstration of NAUTILOS-developed sensors, samplers and systems in a range of different marine conditions, utilising the existing fleet of platforms of opportunity, especially ships of opportunity. The regions used for demonstrations included coastal waters of Norway, the Baltic Sea and the Aegean Sea.

This Deliverable D7.3 provides descriptions of the demonstration actions technical setups for testing the sensors developed in various tasks of WP3 and WP4, and as integrated in WP5 and scenario-tested in WP6.

As the final report of Task 7.2, D7.3 reports the demonstration activities and results of the work carried out by partners from M34 up to M57, illustrates further developments, issues encountered, solutions adopted and data exchange with the NAUTILOS data stream services. Where necessary, D7.3 analyses the data collected in relation to other available validation data. D7.3 assesses the TRL levels of sensors and analyse their fit-for-purpose in platforms of opportunity and, where necessary, provides recommendations for future developments.

D7.3 is organised in nine main sections:

Chapter I introduces the background for the demonstration on platforms of opportunity.

Chapter II contains details of the demonstrations related to drones with multi and hyperspectral cameras and LIF LIDAR.

Chapter III reports details of the demonstrations related to the IR temperature sensor.

Chapter IV contains details of demonstrations related to the sampler for phytoplankton and other suspended matter.

Chapter V gives details of the demonstrations related to the low-cost microplastic sensors based on selective Nile Red staining and fluorescence detection.

Chapter VI reports details of the demonstrations related to the carbonate system/ocean acidification sensors.

Chapter VII contains details of the demonstrations related to the Ferrybox stream data analysis.

Chapter VIII: reports considerations on some ethical aspects relevant to the activities described in this deliverable.

Chapter IX: closes and summarizes the report, highlighting the main achievements obtained in T7.3.

LIST OF FIGURES

Figure 1: The LIF-LIDAR on the Otter Pro ASV during a night deployment showing the deployment configuration and laser beam is visible oriented to the nadir.

Figure 2: Map of demonstration location in Oslofjord (right panel) which is located in southern Norway (left panel). The demonstration location was at Solbergstrand, Norway at NIVA's research station (black star). The MS Color Fantasy Ferrybox planned route passes by NIVA's research station along the dotted red line, but its actual route can depend on metocean conditions. The UAVs were operated in the red rectangular area from the research station to the eastern limit of the Ferrybox route. And the ASV was operated in the dark red box in a relatively close vicinity to the research station.

Figure 3: Simultaneous deployment of a UAV while the MS Color Fantasy is sailing by.

Figure 4: Scheme of one cycle of measurement for one channel. The laser is modulated at 10 Hz, and sampling is performed three times when the laser is on and three times when the laser is off, with the same timing, and for each of the 3 channels. The photodiode (PD) signal is smoother than the laser power, according to its low cutoff frequency.

Figure 5: Calibration of the Chl-a channel with three different algal cultures (left) and the CDOM channel with lignosulfonate (right). The y-axis represents the laboratory spectrophotometric reference measurement while the x-axis displays the LIDAR measurements normalized with Raman signal. Linear correlation coefficients (r^2) of 0.998 on average for Chl-a and 0.987 for CDOM.

Figure 6: Example transect of the hyperspectral camera data overlaid on a map of Oslofjord offshore the NIVA research station with the Ferrybox's sailing path in blue dotted lines on the left side (left panel). Two zoomed in parts of the hyperspectral RGB data are shown including: Top right panel, the region near the research station with seafloor bathymetry visible due to clear nearshore waters as well as some turbid riverine input from a small river that outflow nearby; Bottom right panel, the offshore region close to the Ferrybox route - here sun glint is visible due to sunlight reflection from the wave pattern.

Figure 7: Raw (uncalibrated) images from each channel of the multispectral camera centered at 475 nm (top left panel), 560 nm (top right panel), 668 nm (middle right panel), 717 nm (middle left panel), and 842 nm (bottom left panel), and the spectral signature of the reflectance extracted from pixels averaged in the averaged area represented in red the red squares in each image after calibration (bottom right panel).

Figure 8: Deployment of the LIF-LIDAR on Otter ASV. The survey track has salinity values measured by the miniCT sensor superimposed on top.

Figure 9: Left panel: Matchup between Chl-a measured by the Ferrybox and the reflectances measured by the UAV/multispectral camera; Right panel: Matchup between Chl-a measured by the Ferrybox and Chl-a measured by the UAV/multispectral camera.

Figure 10: Chl-a measurements (mg m^{-3}) of the LIF-LIDAR (orange) and the Turner C3 fluorometer (blue), both mounted to the ASV, during a deployment during night time between 20:34 to 20:46.

Figure 11: Chl-a fluorescence (mg m^{-3}) measured by Turner C3 fluorometer vs LIF-LIDAR.

Figure 12: Chl-a measurements of the LIF-LIDAR (orange), Turner C3 on board of the ASV (grey), Turner C3 onboard the Ferrybox (blue) during a deployment during day time.

Figure 13: The R/V Philia and the IR sensor installed in the left side mast of the ship.

Figure 14: The R/V Philia tracks during the demonstration of the IR sensor.

Figure 15: The CTD control points (highlighted in red) for the validation of the IR sensor data.

Figure 16: Comparison statistics for IR and CTD temperature.

Figure 17: The final dataset visualized in the NAUTILOS data portal.

Figure 18: Sampling track for the Sampler for phytoplankton and other suspended matter on MS Trollfjord from Hjeltefjorden to Ånderdalen/Vangsvik, Norway, in which 19 sampling segments were carried out.

Figure 19: DNA concentrations (ng DNA mL⁻¹ seawater) from samples collected using the automated Sampler (NAUTILOS Sampler, n=19) and manually-collected/filtered samples using a bench top vacuum filtration setup (Manual collection/filtration, n=40).

Figure 20: Installation of the microplastic sampler system on the MS Trollfjord.

Figure 21: The standalone prototype of the combined sampler and oxidation and Nile Red dyeing chamber.

Figure 22: Transects for the analysis of microplastics in Ferrybox samples in 2023.

Figure 23: Left: The custom cuvette and the sensor. Right: The sensors connected in series with the Ferrybox instruments. Photos Sami Kielosto.

Figure 24: Typical cruise track of ferry Finnmaid, including pH measurements presented in colour scale.

Figure 25: Spatiotemporal development of pH in the Baltic Sea from winter 2024 to spring 2025. Data is measured with Endress+Hauser Memosens CPS77E ISFET pH sensor installed onboard ferry Finnmaid. Refer to Fig. 21 for the location of the ship between Helsinki (north) and Travemünde (south). Grey area in the plot indicates when measurements have not been available.

Figure 26: One transect between Helsinki and Travemünde (on 30.4.-1.5.2024) illustrating the large basin-wide variability of pH and how Endress+Hauser Memosens CPS77E ISFET pH sensor (black) and Contros HydroFIA (red) disagree with the measurement scales, but agree with range of variability. The insert in the right upper corner zooms in the southernmost part of the transect and illustrates how sensors read similarly the small-scale variations in pH.

Figure 27: Relationship between Endress+Hauser Memosens CPS77E ISFET pH sensor and Contros HydroFIA pH sensor measurements. Black line is 1:1 fit. For the whole range, the difference is approximately 0.4 pH units.

Figure 28: The difference between Endress+Hauser Memosens CPS77E ISFET pH sensor and Contros HydroFIA pH sensor measurements against water temperature, showing a slight increase of difference as water warms up (see also Fig. 26, as this may have been related to the sensor drift as function of time).

Figure 29: The difference between Endress+Hauser Memosens CPS77E ISFET pH sensor and Contros HydroFIA pH sensor measurements against the date (from March 2024 to August 2024) showing a slight increase of difference possibly related to sensor drift.

Figure 30: Drift of Endress+Hauser Memosens CPS77E ISFET pH sensor installed in ferry Finnmaid. Sensor was calibrated 21.10.2024 and calibration was followed using buffer solutions.

Figure 31: Spatiotemporal distribution of the annotated algal bloom events.

Figure 32: Pareto front of the fitted models. Best trials highlighted in red. Colour saturation indicates number of the trials.

LIST OF TABLES

Table 1: Sampling locations and supporting data for the Sampler for phytoplankton and other suspended matter including station number (TF1-19), approximate geographical/coastal region, date, time, longitude (Long), latitude (Lat), Chl-a fluorescence (Chl-a flu), sea surface temperature (Inlet temp), and salinity.

Table 2: Detailed information on the 15 transect sampled during the 2023 sampling campaign on the MS Trollfjord.

LIST OF ACRONYMS AND ABBREVIATIONS

Abbreviation	Definition
4G	Fourth-Generation of cellular network technology
5G	Fifth-Generation of cellular network technology
ADC	Analog to Digital Converter
AI	Artificial Intelligence
ASV	Autonomous Surface Vehicle
AUV	Autonomous Underwater Vehicles
CDOM	Coloured dissolved organic matter
Chl-a	Chlorophyll a
CSV	Comma Separated Value
CTD	Conductivity, Temperature, and Depth
DNA	Deoxyribonucleic acid
DC	Direct Current
eDNA	Environmental DNA
EMI	Electromagnetic Interference
EOV	Essential Ocean Variable
EtOH	Ethanol
EuroGOOS	European component of the Global Ocean Observing System
fANOVA	Functional Analysis of Variance
fDOM	Fluorescent part of Coloured Dissolved Organic Matter
FTP	File Transfer Protocol
GNSS	Global Navigation Satellite System

GPS	Global Positioning System
IR	Infrared
ISFET	Ion-Sensitive Field-Effect Transistor
IMU	Inertial Measurement Unit
JERICO-S3	Joint European Research Infrastructure of Coastal Observatories: Science, Service, Sustainability
KNN	k-Nearest Neighbors
LIF LIDAR	Laser-Induced fluorescence Light Detection And Ranging
LOD	Limit of Detection
LOQ	Limit of Quantification
LTE modem	Long Term Evolution modem
MP	Microplastic
MS	Motor Ship
NORCCA	Norwegian Culture Collection of Algae
PD	Photo Diode
PES	Polyethersulfone
PPS	Particle and Phytoplankton Sampler
PSU	Practical Salinity Unit
PVC	Polyvinyl chloride
pyr-GC/MS	Pyrolysis–gas chromatography–mass spectrometry
QC	Quality Control
RGB	Red-Green-Blue
RPM	Rounds Per Minute
RS232	Recommended Standard 232
RTU	Remote Terminal Unit
R/V	Research Vessel
SGD	Stochastic Gradient Descent
SME	Small- and Middle-size Enterprise
SSH	Secure Shell Protocol
T	Temperature
TRL	Technology Readiness Level
UART	Universal Asynchronous Receiver/Transmitter
UAV	Unmanned Aerial Vehicle
USB	Universal Serial Bus
UTC	Coordinated Universal Time
UV	Ultraviolet
VOOs	Vessels Of Opportunity
VSC	Vehicle Control Station
WP	Work Package
μFTIR	micro Fourier Transform Interferometer

I. INTRODUCTION

NAUTILOS Horizon 2020 project has developed a series of cost-efficient sensors and samplers to fill in the existing gaps in marine observations. Project includes all the key steps when increasing the Technology Readiness Level (TRL) of the sensors - development, integration, validation and demonstration - including different expert groups, with complementary skills, for each step.

To describe the process briefly, WP2 targeted the overall technological requirements to meet the needs of ocean observing, facilitated interoperability and provided overall guidelines to all technologies to be developed. The actual technological developments of sensors have been done in WP3&4. The main engineering, done by experts in SMEs and research laboratories, was supported by the oceanographic members of partnership who have provided their feedback during the development work to ensure fit-of-purpose of new sensors. Next step in WP5 was integration of sensors to the predefined measuring platforms like benthic landers and AUVs, or to Ferrybox ships of opportunity which is the main topic of D7.3. The aim of this integration work was to find solutions for physical, electrical and software integration, and validate that sensors work in a given platform. NAUTILOS Deliverable 5.6. specifically reports the integration of sensors and samplers on Ferrybox Ships of Opportunity. WP6 provided validation of sensors and samplers in controlled environments, and where needed, provided calibration and validation of their performance. The validation tests of the sensors considered in this document have been documented in NAUTILOS Deliverables D6.1-D6.5. These prior NAUTILOS deliverables can be found at <https://nautilus-h2020.eu/results/deliverables/>.

Ferrybox measurements using ships of opportunity have been conducted since the 1990s and typically the measurements include variables like temperature, salinity and fluorescence, other more advanced sensors being added recently (e.g., Petersen 2014). Ferrybox systems usually have no practical limitation for power consumption and large sensors can be used. On the other hand, measurements need to be done in flow-through mode, using some kind of flow-caps. Basic setups and best practices for Ferrybox measurements are given by Petersen and Colijn (2017) and Mantovani et al. (2023).

NAUTILOS sensors for Ferryboxes take a step forward in providing new types of possibilities for ocean observing. They target emerging environmental challenges (plastic pollution, carbonate system dynamics), much-awaited possibilities to collect and fix samples in an automated way, and measuring surface water properties using close-range sensing technologies, well suited e.g., for satellite data validation, and also applicable to be used in aerial platforms, as also demonstrated in this task using drones.

The sensors tested in Task 7.2, using platforms of opportunity, included

- Drones with multi and hyperspectral cameras; LIF LIDAR (Chapter II)
- The IR temperature sensor (Chapter III)
- Sampler for phytoplankton and other suspended matter (Chapter IV)
- Low-cost Microplastic sensors based on selective Nile Red staining and fluorescence detection (Chapter V)
- Carbonate system/ocean acidification sensors (Chapter VI)

The work was complemented with Ferry Box Stream Data Analysis (Chapter VII)

II. DRONES WITH MULTI- AND HYPER-SPECTRAL CAMERAS AND LIF LIDAR. DEMONSTRATION REPORT (NIVA)

1. BACKGROUND

Several downward-looking sensors for ocean platforms and aerial drones were developed within Task 3.2 of NAUTILOS. These included a multispectral camera, a hyperspectral camera, and a Laser-Induced Fluorescence Light Detection And Ranging (LIF-LIDAR) sensor for measuring ocean colour including chlorophyll a (Chl-a) and coloured dissolved organic matter (CDOM) and other applications. These sensors, when integrated on opportunistic and flexible observing platforms like autonomous surface vehicles (ASVs) and aerial drones (unmanned aerial vehicles; UAVs), can complement traditional ocean observing platforms that usually provide observations at fixed points or along fixed routes. The utilisation of ASVs and UAVs can also facilitate observations of coastal regions (or deployed in the vicinity of ships) that otherwise are difficult to access or altogether inaccessible. The use of downward-looking sensors from UAVs also allows for *ex situ* ocean observations that can increase the spatial extent and targeted nature of observations. The sensors were tested in a lab setting and reported in Deliverable 3.3 and integrated on ASV and aerial drones (UAVs) which were reported in Deliverables 5.2 and 5.4, respectively. Calibration and validation tasks were carried out in WP6 and the laboratory-based calibrations of the cameras/LIF-LIDAR were reported in Deliverable 6.1 while the field validation with operation on observing platforms were reported in Deliverable 6.5.

2. DEMONSTRATION PLAN

The multi- and hyper-spectral cameras and the LIF-LIDAR were demonstrated in Oslofjord at Solbergstrand, Norway where NIVA's field research station is located. The UAVs and ASV were launched from the shore and made observations that crossed the MS Color Fantasy Ferrybox's path just before it passed. The demonstration was also timed to coincide with Sentinel 2/3 and Landsat 8/9 satellite passes for remote sensing matchups which are reported in more detail in Deliverable 9.4. The LIF-LIDAR instrument was initially planned to be installed on the same ship operating a Ferrybox, but due to eye safety concerns of passengers and finding a suitable location on the ship, it was instead deployed on an ASV also in Oslofjord from NIVA's field research station. The LIF-LIDAR ASV demonstrations took place both at night and during day to compare its performance under varying background light conditions.

Demonstration on UAVs and ASV in the Norwegian Coastal Seas

- **Specific Objectives**

The primary objective of the demonstration was to showcase the capabilities and complementarities of the NAUTILOS instruments and platforms under real-world environmental conditions in coordinated operations near an active Ferrybox route that made observations for ground-truthing.

Specifically, the demonstration assessed:

- The ability of multi-spectral and hyper-spectral cameras on UAVs to effectively capture high-resolution spatial data along the Ferrybox's path.

- The operational performance of a LIF-LIDAR deployed on an ASV, particularly in terms of data quality under both daylight and nighttime conditions.
- The capabilities for long term and high temporal resolution of Ferrybox data for training of AI algorithms for early event detection (results Section VII “Ferry Box Stream Data Analysis Demonstration Report” of this Deliverable)

These objectives support the broader goals of NAUTILOS to enhance autonomous in situ and remote sensing capabilities for marine environmental monitoring.

- **Platforms involved**

Three types of platforms were involved in this demonstration: UAVs, ASV and Ferrybox. The platforms will be described briefly below, and more detailed information can be found in Deliverables 5.4 and D5.2, respectively.

DJI Matrice 300 RTK and Matrice 600 Pro UAVs

The multispectral and hyperspectral cameras were deployed on two different multirotor UAVs, a DJI Matrice 300 RTK, and a DJI Matrice 600 Pro.

The DJI Matrice 300 is a high performance reliable and versatile commercial multirotor (four rotors) UAV with up to 55 min of flight. It is approximately 1m*1m, has a maximum payload of 2.7 kg and is compatible with numerous models of attachments and gimbals. It also allows the use of up to 3 brackets/gimbals at the same time, one upward looking and 2 downward looking. The DJI Matrice 300 is powered by 2 batteries of 46.2 V and 5935 mAh in parallel. The DJI Matrice 300 RTK is used to deploy the Micasense Altum multispectral camera. The multispectral camera can also be combined with an RGB camera, as the DJI Matrice 300 had a double gimbal.

The DJI Matrice 600 Pro is a 1.5 m multirotor (six rotors) UAV, capable of carrying up to 6kg, and flying up to 18 m s⁻¹. Its high payload capacity enables it to operate with the hyperspectral camera, which weighs over 4 kg with its gimbal. The DJI Matrice 600 Pro is powered by 6 batteries of 22.8 V 5700 mAh coupled in pairs to provide 46 V to the motors. Its autonomy is 15 minutes with its maximum payload and its maximum autonomy is ~30 min. The DJI Matrice 600 Pro is mainly used to deploy the Specim AFX10 hyperspectral camera.

Maritime Robotics Otter Pro ASV

The ASV is an Otter Pro from Maritime Robotics (Fig. 1). It is a twin-hull vessel, 2 m long, 1 m wide, and weighs 60 kg. Its control systems, payload sensors and two rear thrusters are powered by four 1 kWh Li-ion batteries which enable an operational range of ~20 hours (depending on speed and payload). The Otter Pro has a high-quality IMU and dual GNSS antenna navigation and control system, which means that a mission pattern can be preprogrammed, and can be monitored and controlled over three different channels: Wi-Fi (200 m range), 5 GHz broadband radio communication (2 km range), or 4G. When in operation, the ASV follows pre-programmed survey patterns and must be operated with care, as it does not have any obstacle detection/avoidance capabilities. There is, however, a forward-facing camera that provides the operator with a live video feed to monitor operations and potential collision hazards. The Otter Pro is configured, monitored, and controlled via the manufacturer’s VCS (Vehicle Control Station) software on Linux or Android. For the test deployment the sensor payload comprised of a BioSonics MX aquatic habitat, 200 kHz single-beam echo sounder with 100 m range, a Valeport MiniCT conductivity- and

temperature sensor, and a Turner Designs C3 optical sensor for turbidity, Chl-a fluorescence, and CDOM fluorescence, measuring at approximately 15 cm under the surface of the water.

MS Color Fantasy Ferrybox

NIVA operates a Ferrybox system installed on board the MS Color Fantasy, operated by Color Line and sailing between Oslo, Norway and Kiel, Germany. The Ferrybox passes by the demonstration site every other day as it takes two days to complete a roundtrip from Oslo-Kiel-Oslo. The system pumps water at 4 m depth and continuously measures various oceanographic parameters including salinity, temperature, Chl-a fluorescence, CDOM fluorescence, turbidity, dissolved oxygen, and carbonate system variables.

- **Deployment configuration**

The integration and deployment configuration of the sensors and platforms in this demonstration consisted of the Micasense Altum multispectral camera on the DJI Matrice 300 RTK UAV, the Specim AFX10 hyperspectral camera on the DJI Matrice 600 Pro UAV, and the LIF-LIDAR on the Maritime Robotics Otter Pro. The Micasense Altum multispectral camera was mounted with a Skyport dampening bracket, the Specim AFX10 hyperspectral camera was attached to via a Gremsy T7 3-axis Digital Gyro-Stabilised Gimbal, and the LIF-LIDAR was attached to the mid-section of the Otter Pro with a custom-made bracket. Photos of the deployment configuration of the cameras and UAVs can be found Deliverable 5.4, and a photo of the LIF-LIDAR with the Maritime Robotics Otter Pro is shown in Fig. 1.

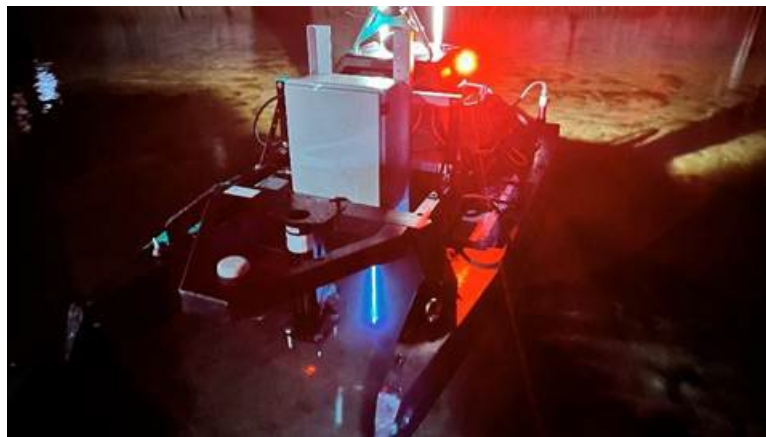


Figure 1: The LIF-LIDAR on the Otter Pro ASV during a night deployment showing the deployment configuration and laser beam is visible oriented to the nadir.

- **Location**

The UAVs and ASV with their respective sensors were deployed from NIVA's research station at Solbergstrand, Norway (approximately 40 km south of Oslo, Norway; 59.62 °N, 10.65 °E) in the Oslofjord where the MS Color Fantasy Ferrybox operates (Fig. 2 and 3).

- **Period of occurrence**

The sensors were deployed synchronized with ferry passes in May 2023 and July 2024 for the hyperspectral and multispectral cameras, and in September 2024 with the multispectral camera and the LIF-LIDAR.

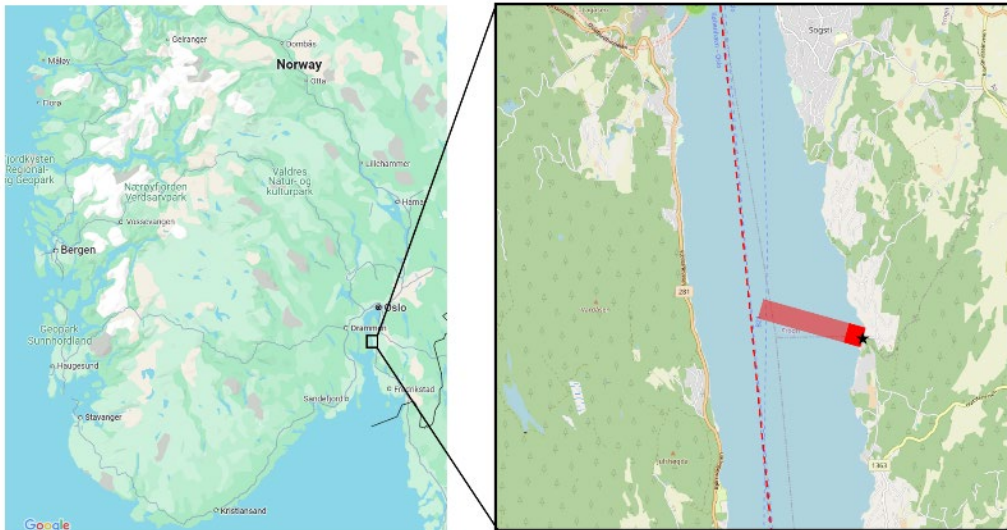


Figure 2: Map of demonstration location in Oslofjord (right panel) which is located in southern Norway (left panel). The demonstration location was at Solbergstrand, Norway at NIVA's research station (black star). The MS Color Fantasy Ferrybox planned route passes by NIVA's research station along the dotted red line, but its actual route can depend on metocean conditions. The UAVs were operated in the red rectangular area from the research station to the eastern limit of the Ferrybox route. And the ASV was operated in the dark red box in a relatively close vicinity to the research station.



Figure 3: Simultaneous deployment of a UAV while the MS Color Fantasy is sailing by.

- **Maintenance, events/issues occurred and actions taken**

No maintenance needed nor issues encountered. Some weather delays during the demonstration period limited some UAV operations (poor flying conditions) as well as some satellite data matchups due to cloud cover.

- **Data recovery/ Analysis**

Cameras:

For both hyperspectral (Specim AFX10) and multispectral (Micasense Altum) cameras, the raw data, i.e., uncalibrated images are stored in internal memory and recovered after each deployment. The data analyses are performed after offloading the data as follows:

First, calibrations are applied on the raw data to correct for geometric aberrations introduced by the optics of the systems such as vignetting and roll-off. These geometrical characterizations were performed by the manufacturers and calibration files were provided with the instruments.

Then the dark signal from the raw image (mean value of the dark pixels) was removed and the signal was normalised with the exposure time, and calibration coefficients were applied to convert the raw values into absolute radiance. This data processing stream was also applied for images taken of a calibration panel during the demonstration. The calibration panel is a reflective surface of a known reflectivity, and cameras are flown over this calibration panel before every flight and the mean radiance value of the calibration panel is extracted. A coefficient is then calculated from the ratio between the theoretical reflectance and the mean value of the reflectance and is then used to calculate the reflectance from the measured radiance during the flight.

While the multispectral sensor has its own white calibration target, for the hyperspectral camera, and for water quality monitoring applications in general, it can be helpful to calibrate the sensors with an in-scene calibration target with a reflectance closer to the target application. Otherwise, the sensitivity level in the target application may be too low. Two calibration tarps were used for this purpose, one with a reflectance of 0.48 and the other with a reflectance of 0.063. The empirical line method is used to calibrate the reflectance for in-scene targets. It is challenging to find a reflectance standard as dark as water. Therefore, optimal performance for water quality monitoring has been found to be achieved with the 0.063-reflectance tarp combined with an additional technique for removing the dark current from the data. For the AFX10 hyperspectral camera, the dark current is estimated automatically in each mission, as the shutter of the camera is closed for the last 100 frames. After calibration and georeferencing, ocean colour algorithms can then be applied using reflectance data to retrieve the concentration of seawater constituents of interest.

LIF-LIDAR:

The sensor operates autonomously with respect to software and data storage via a Raspberry Pi4. The system receives operational commands via a python-based software running on the Raspberry Pi 4. The software has a PyQt5 based graphical interface for data visualisation and logs the data internally on a micro-SD memory card. The software is licensed under the ApacheMIT license, version 2.0 and freely available.

Each measurement consists of a cycle of two steps: fluorescence signal collection and background signal collection. For the first step, the laser is turned on, and after a short waiting period to allow the signal of the photodiode to stabilize, the signal is measured three times on each of the three channels, and averaged. Then, during the second step, the laser is turned off, and after another waiting period for photodiode stabilization, the background signal is also measured three times per channel and averaged. The stabilization time is necessary due to the photodiode's transient response, dark current stabilization, and thermal effects, which can cause fluctuations in the signal immediately after switching the laser on or off. The final measurement is obtained by averaging the data from five cycles, subtracting the background

signal from each respective channel, and normalising the Chl-a and CDOM channels with the Raman signal. Fig. 4 shows the sequence of measurement for one channel. A calibration coefficient is then applied to the fluorescence measurements to convert it to concentration. The calibration is described in the other related activities section below.

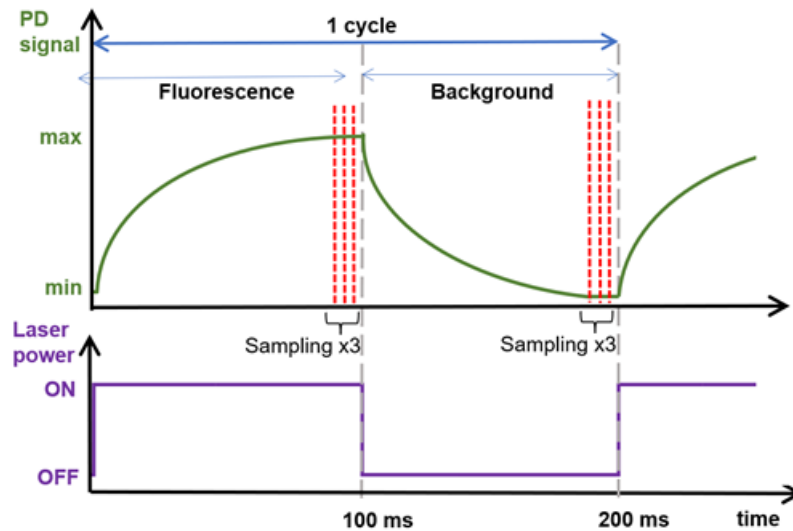


Figure 4: Scheme of one cycle of measurement for one channel. The laser is modulated at 10 Hz, and sampling is performed three times when the laser is on and three times when the laser is off, with the same timing, and for each of the 3 channels. The photodiode (PD) signal is smoother than the laser power, according to its low cutoff frequency.

The data are analysed at the time of measurement and the sensor was equipped with a 4G router, so data were available in real-time for visualisation or download and could also be transferred after each mission after recovery of the instrument.

- **Other Relative Activities**

LIF-LIDAR absolute calibration

As the LIF-LIDAR provides the fluorescence signal of Chl-a and CDOM normalized by the water Raman signal, it takes into account fluctuations in the laser power, changes in the geometry of the collection (e.g., distance from the water, reflection from water/air interface) as well as changes in the water extinction (i.e., turbidity). However, this value needs to be associated to Chl-a or CDOM concentrations through a calibration process, therefore an extended laboratory calibration was performed prior to first deployment at sea using various concentrations of three different algal cultures for Chl-a, and lignosulfonate for CDOM, in addition to the first set of characterizations and calibration of the optics and electronics performed in WP6 and described in Deliverable 6.1.

Three different types of algal cultures from the Norwegian Culture Collection of Algae (NORCCA) were used for Chl-a fluorescence-to-mass calibration of the instrument: a green algae *Tetraselmis* sp. (NIVA-6/06) and two species of diatoms: *Pheodactylum tricornutum* (NIVA-BAC2) and *Skeletonema pseudocostatum* (NIVA-BAC1). These species were chosen as *S. pseudocostatum* is one of the most abundant microalgae in the Oslofjord (Paasche and Ostegren, 1980), where the sensor was to be first deployed. *Tetraselmis* sp. appears bright green due to its high chlorophyll a and b content, typical of green algae (Chlorophyta). In

contrast, the diatoms, *P. tricornutum* and *S. pseudocostatum* show golden-brown hues, a characteristic of their dominant accessory pigment, fucoxanthin, along with Chl-a and -c. As for the calibration for CDOM, a solution of lignosulfonate (Borregaard FP-P, Batch 91900833), a soluble form of lignin, the natural plant polymer, was used to simulate CDOM due to its optical properties, similar to natural CDOM with strong UV-visible absorption and fluorescence.

The algal cultures or the lignosulfonate solution were diluted with seawater to produce a range of different concentrations. The seawater was collected from the nearby fjord at 60 meters depth, just offshore of the research facility. The seawater had a salinity of 32 PSU and its total suspended matter concentration was under 1 mg L⁻¹. The dilutions were placed in a 120 L tank with black walls and equipped with a peristaltic pump for water circulation, sampling and online measurements of CDOM fluorescence (fDOM) and Chl-a fluorescence with a Turner C3 fluorometer. The C3 measurements were converted into Chl-a concentration and quinine sulphate unit equivalents through a pre-calibration. The instrument was placed 5 m away from the middle of the tank and was set horizontally, with its beam directed to the tank with a flat mirror at 45°. The reference Chl-a values were measured spectrophotometrically from water samples filtered with Ø 47 mm GF/F filters. The pigments were then extracted in a 100 % methanol solution and analysed on a Perkin Elmer UV/VIS Lambda 365 spectrophotometer, following Norwegian NS-4767 protocol. With respect to CDOM calibration samples were filtered through Ø 47 mm 0.2 µm pore size Nucleopore filters for each dilution, and the absorbance of the filtrate was measured spectrophotometrically and converted in absorption.

The LIF-LIDAR recorded for ~90 seconds (~45 measurements) for each sample. The measurements of each sample were then averaged, after background removal for each measurement and normalization with corresponding Raman observation.

The laboratory calibrations demonstrated very good performance of the instrument; the background removal corrected eventual drift caused by illumination variation during sampling and the Raman normalization compensated eventual fluctuations caused by variation in water attenuation or potential laser power variation. The variability of the sensor during the calibration exercise was 2.5% for the Raman channel and 3.1% and 4.6% for the Chl-a and CDOM channels, respectively. Furthermore, excellent linearity and sensitivity was found for both the Chl-a and CDOM channels (Fig. 5; $r^2=0.998-1.00$ for Chl-a and $r^2=0.987$ for CDOM). As expected, the system showed higher sensitivity to *Tetraselmis sp.*, which contains the highest concentration of Chl-a and for which the detection was specifically optimized. The LIF-LIDAR measurements also showed very good agreement with both Chl-a and fDOM measured with the Turner C3 fluorometer (results not shown), as well as with the absorptions at 440 nm measured with the benchtop spectrophotometer.

For the first deployment of the sensor, the results from laboratory tests were used, and the calibration coefficients of *S. pseudocostatum* versus spectrophotometric reference measurements were applied to the Chl-a signal, as it is among the most commonly occurring species in the Oslofjord. For future deployments, accuracy could be improved by calibrating the sensor prior to each mission using natural water samples, which can be concentrated through refiltration for both Chl-a and CDOM measurements.

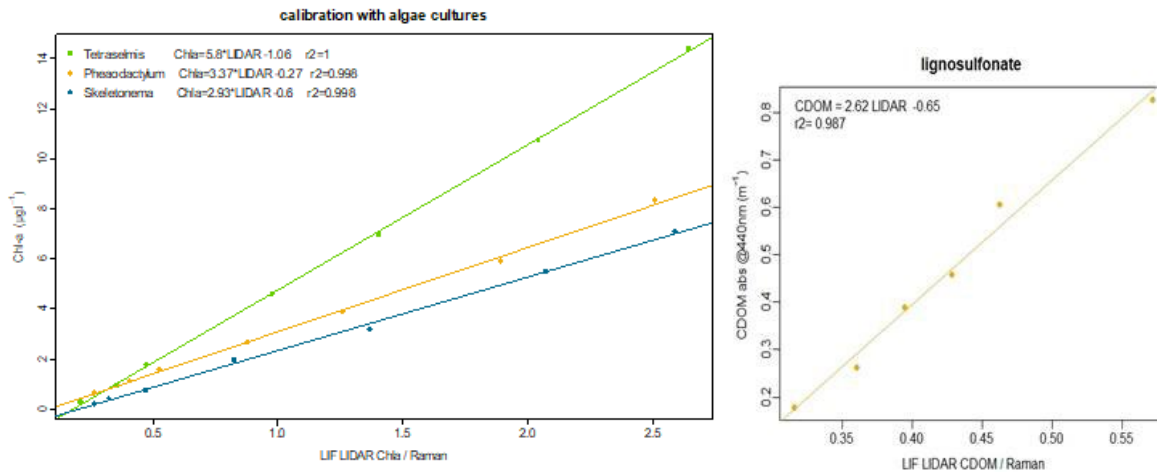


Figure 5: Calibration of the Chl-a channel with three different algal cultures (left) and the CDOM channel with lignosulfonate (right). The y-axis represents the laboratory spectrophotometric reference measurement while the x-axis displays the LIDAR measurements normalized with Raman signal. Linear correlation coefficients (r^2) of 0.998 on average for Chl-a and 0.987 for CDOM.

Remote sensing

Data collected by all the sensors during this demonstration were used for validation for remote sensing in Task 9.4 and reported in Deliverable 9.4.

Event detection

In connection with UAV and Ferrybox demonstration, AI-based event detection algorithms were developed by DFKI using two years of annotated data from MS Color Fantasy Ferrybox data acquired (section VII below). Additional event detection-related activities for Aquaculture Observing Systems are reported in Deliverable 7.2.

3. RESULTS – COMMENTS – CONCLUSIONS

● Results

The cameras, along with their respective UAV platforms, were successfully deployed in the field and operated as expected throughout the data collection campaigns. They consistently captured high-quality imagery, demonstrating reliable performance under various wind/weather conditions. The cameras successfully collected and stored data throughout their flights. The sampling transect for the hyper- and multispectral cameras with UAVs are shown in Fig. 2. In total, 44 multi- and hyper- spectral datasets were collected at NIVA's research station, including 5 multispectral data transects and 4 hyperspectral data transects during the demonstration. The transects covered surface waters between the NIVA field station and the MS Color Fantasy Ferrybox sailing path. An example of RGB image data collected by the DJI Matrice 600 Pro and Specim AFX10 hyperspectral camera is shown in Fig 6. The raw data obtained from the multispectral and hyperspectral cameras will be used for subsequent analysis and algorithm application in Task 9.4, validating the overall system design and integration.

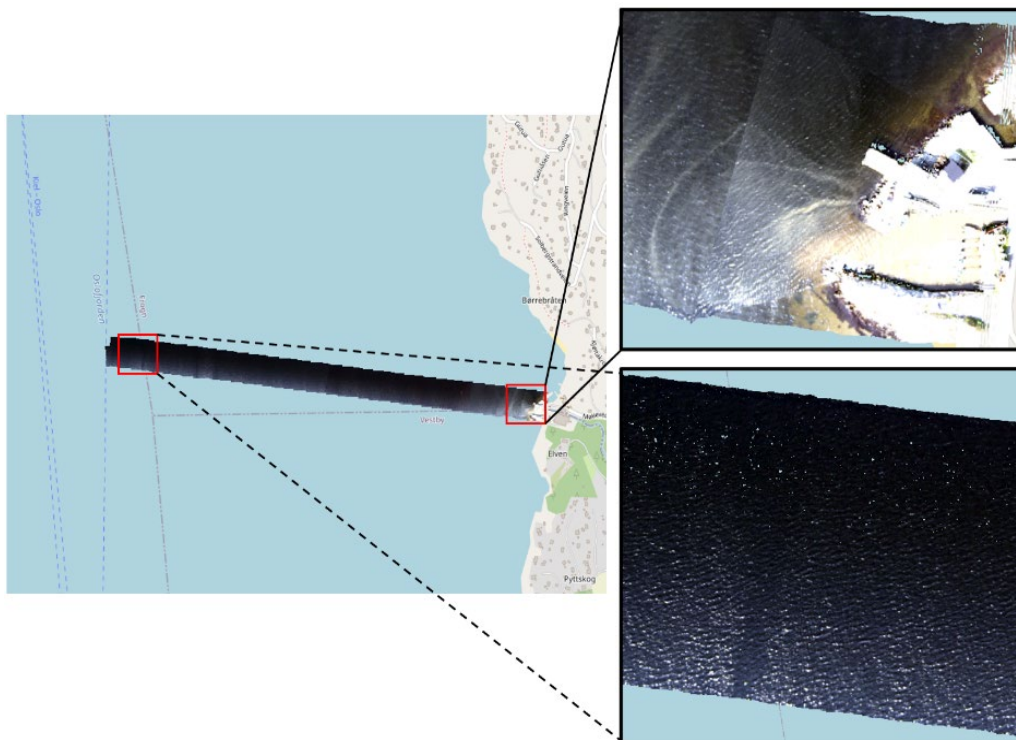


Figure 6: Example transect of the hyperspectral camera data overlaid on a map of Oslofjord offshore the NIVA research station with the Ferrybox's sailing path in blue dotted lines on the left side (left panel). Two zoomed in parts of the hyperspectral RGB data are shown including: Top right panel, the region near the research station with seafloor bathymetry visible due to clear nearshore waters as well as some turbid riverine input from a small river that outflow nearby; Bottom right panel, the offshore region close to the Ferrybox route - here sun glint is visible due to sunlight reflection from the wave pattern.

The strong signal across the spectrum of the reflectances (Fig.7) shows strong backscattering indicating high particle concentration. This scene was captured directly outside of NIVA's marine station the 05/09/2024 the day after the LIF-LIDAR passed through the same location (Fig. 8).

Reflectance data were also extracted from transect over the fjord with the same method and were matched with passes of NIVA's Ferrybox system onboard the MS Color Fantasy. First the ratio between Blue to green reflectance signal was compared to the Chl-a concentration measured with a C3 fluorometer (calibrated with Chl-a samples), showing a good correlation as shown in Fig 9 (left panel). The coefficients derived from the calibration and validation exercise using a large outdoor tank presented in Deliverable 6.1 were then applied to the reflectance to convert the reflectance values to Chl-a concentration and compared to the Chl-a concentration measured from the Ferrybox (Fig 9; right panel). While the UAV data tended to overestimate Chl-a concentrations, the correlation remained good. The observed offset is likely due to the limited dynamic range of Chl-a concentrations in natural waters, in contrast to the broader range created in the controlled tank environment used for validation. Additionally, the Ferrybox measures Chl-a in seawater pumped in from an inlet at ~4 m depth, while the UAV and multispectral camera is integrating reflectance signals from the euphotic depth. To improve the accuracy and robustness of the inversion algorithm used to retrieve Chl-a concentrations, a larger number of observations in diverse natural conditions is recommended.

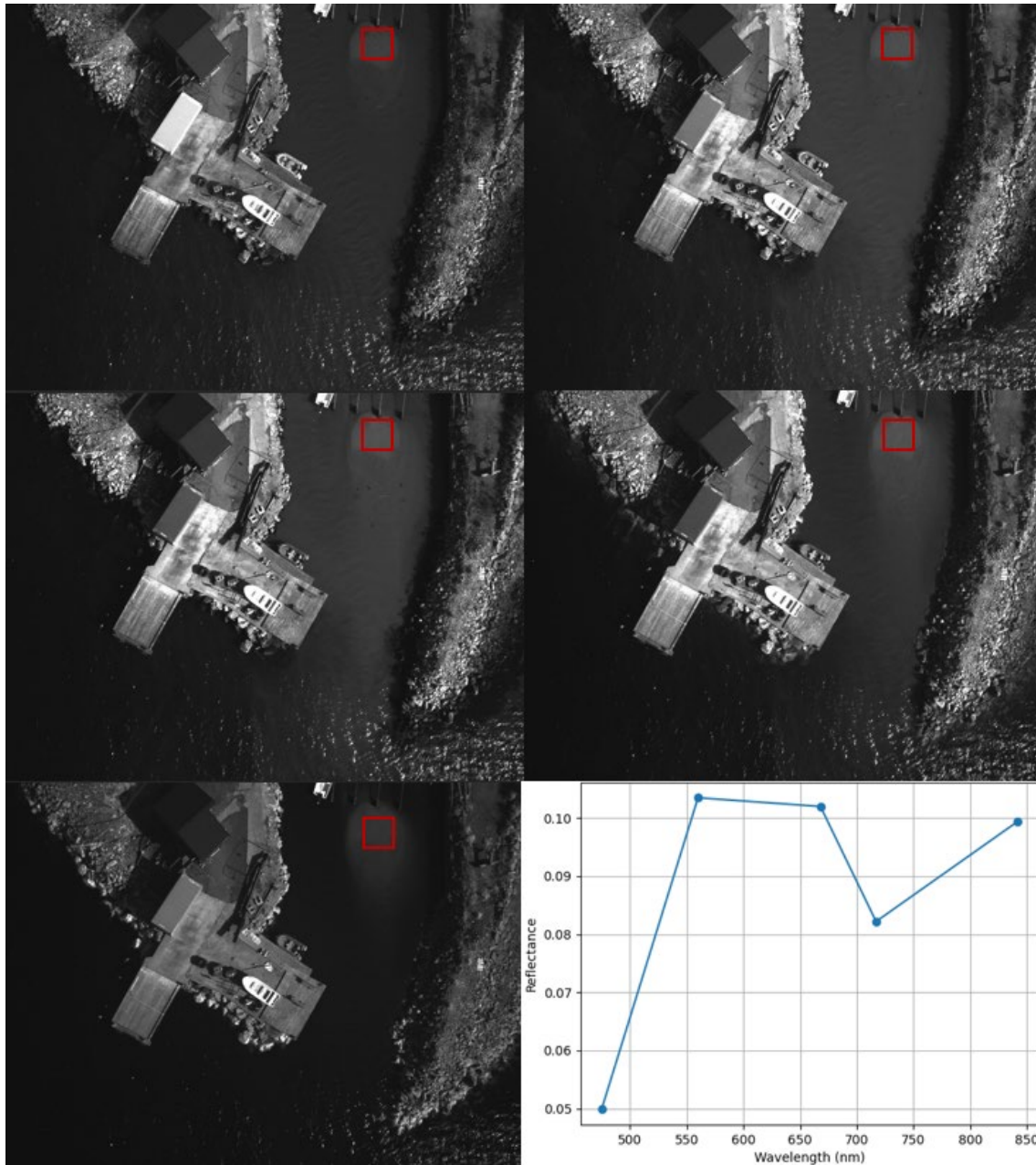


Figure 7: Raw (uncalibrated) images from each channel of the multispectral camera centered at 475 nm (top left panel), 560 nm (top right panel), 668 nm (middle right panel), 717 nm (middle left panel), and 842 nm (bottom left panel), and the spectral signature of the reflectance extracted from pixels averaged in the averaged area represented in red the red squares in each image after calibration (bottom right panel).

The LIF-LIDAR with ASV consistently demonstrated robust performance and operational reliability, effectively withstanding the challenging and variable conditions encountered in the marine environment during sea deployments. Throughout the measurement campaigns, it maintained stable functionality with minimal downtime or technical interruptions, ensuring continuous data acquisition. The ASV performed a diamond-shaped survey during the daytime as well as an “out-and-back” survey during the nighttime with the LIF-LIDAR (Fig. 8). Comparative analysis with the subsurface Turner C3 fluorometer (a conventional Chl-a fluorescence measuring technique) mounted to the hull of the ASV showed strong

agreement, confirming the system’s accuracy and precision in measuring chlorophyll-a concentrations (Figs. 10 and 11).

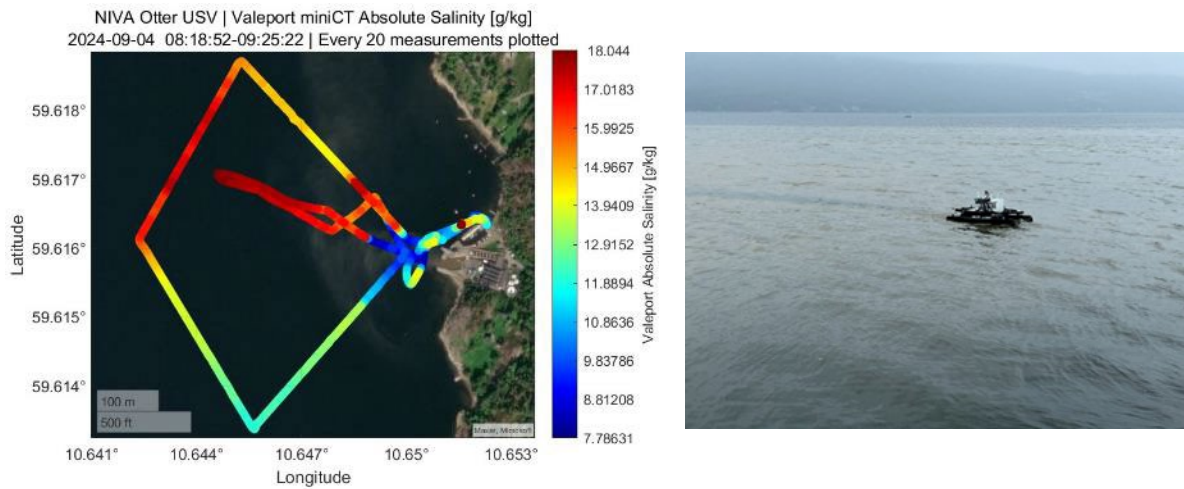


Figure 8: Deployment of the LIF-LIDAR on Otter ASV. The survey track has salinity values measured by the miniCT sensor superimposed on top.

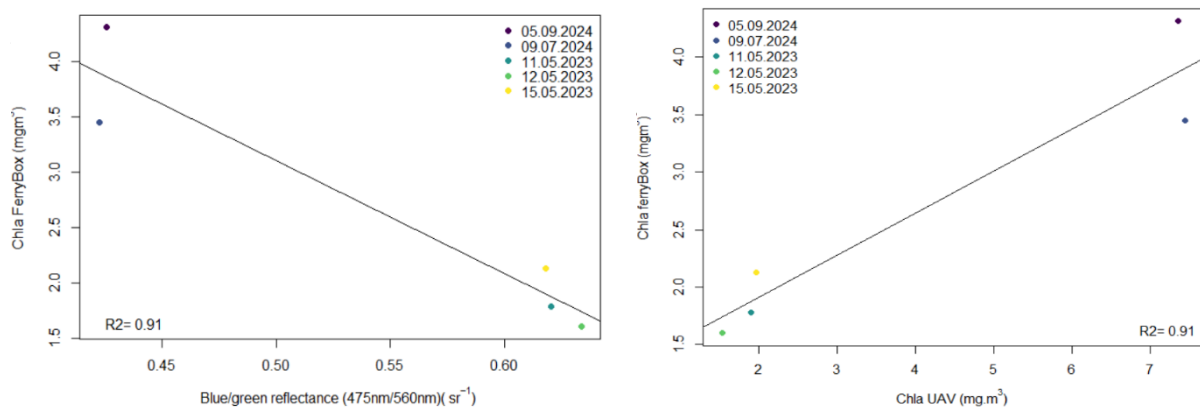


Figure 9: Left panel: Matchup between Chl-a measured by the Ferrybox and the reflectances measured by the UAV/multispectral camera; Right panel: Matchup between Chl-a measured by the Ferrybox and Chl-a measured by the UAV/multispectral camera.

The LIF-LIDAR data was also evaluated from when it was deployed during daytime just before the Ferrybox pass. Data from the LIF-LIDAR and Turner C3 fluorometer on board of the ASV were compared to the Turner C3 Chl-a fluorescence installed onboard of the Color Fantasy Ferrybox (Fig.12).

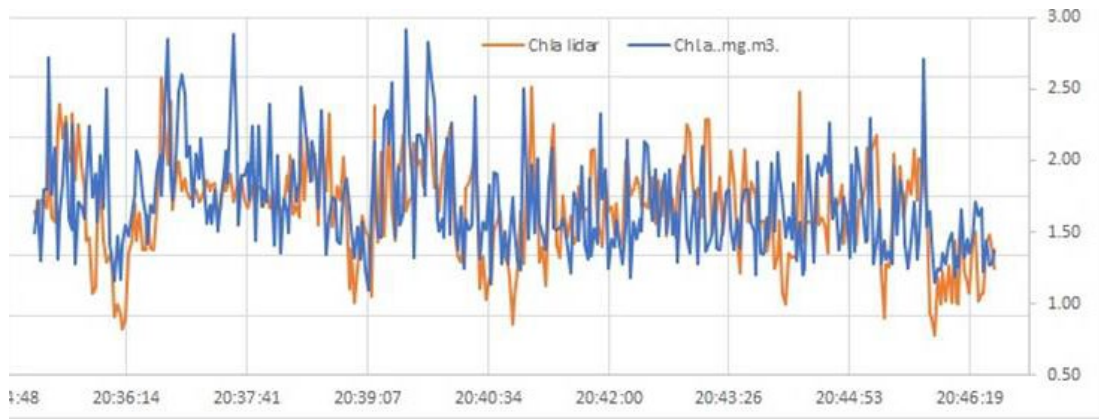


Figure 10: Chl-a measurements (mg m^{-3}) of the LIF-LIDAR (orange) and the Turner C3 fluorometer (blue), both mounted to the ASV, during a deployment during night time between 20:34 to 20:46.

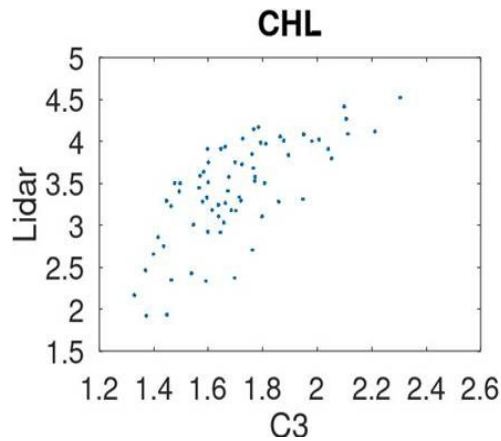


Figure 11: Chl-a fluorescence (mg m^{-3}) measured by Turner C3 fluorometer vs LIF-LIDAR.

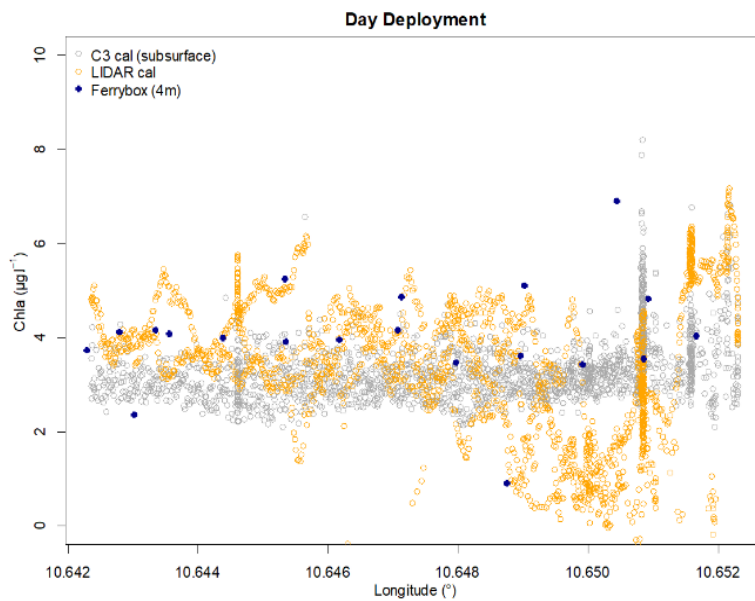


Figure 12: Chl-a measurements of the LIF-LIDAR (orange), Turner C3 on board of the ASV (grey), Turner C3 onboard the Ferrybox (blue) during a deployment during day time.

- **TRL achievement level and project SOP**

Based on the successful collection of data in “real conditions” the sensors have reached a TRL of 7. Sensor and platform prototypes (cameras with UAVs and LIF-LIDAR with ASV) were demonstrated and tested in the marine environment based on realistic operating conditions and successfully measured Chl-a and CDOM concentration consistent with conventional measurements made using a Ferrybox platform and fluorometers.

- **Future plans and Recommendations**

Although the cameras and their UAV platforms are currently fully operational as standalone technologies (as commercial off the shelf equipment), the performance and applicability of ocean colour algorithms remain highly dependent on both the sensor characteristics and the specific environmental conditions of the region, as well as the integration of the sensors with various platforms. To enhance the robustness and accuracy of water quality parameter retrievals from the camera measurements, it is essential to collect large and diverse datasets. Future efforts should therefore focus on acquiring extensive observations across a variety of aquatic environments and under different atmospheric and lighting conditions. Additionally, ground-truthing with *in situ* and satellite remote sensing products will provide additional observations to fill in spatial and temporal gaps in ocean observations.

As for the LIF-LIDAR, current investigations aim to improve signal quality by implementing high-pass filters or lock-in detection to suppress continuous background signals across all three channels. Hardware improvements under consideration include extending the ADC dynamic range to 12 V—aligning with the photodiode saturation level—and integrating low-cost lock-in amplifiers to enhance daytime performance. Future developments will explore both the miniaturisation of the system and the creation of an extended profiling version, enabling vertical distribution measurements. Additional applications under investigation include detection of other fluorescent targets such as oil spills, microplastics, and organic pollutants, as well as integration on diverse autonomous or remotely operated platforms. Further deployments are planned to more comprehensively assess the instrument’s performance across varying environmental conditions. Beyond its use on ASV, including also long-distance autonomous platforms such as surface or wave gliders, the sensor can also be integrated into a wide range of platforms. These include ships of opportunity, as initially planned, but preferably on cargo vessels, where laser safety considerations may not limit deployment unlike on passenger ferries, as well as moored platforms, bridges, pontoons, or other fixed installations. The flexibility of above water deployments offers promising avenues for extending observation capabilities across diverse marine environments.

III. IR TEMPERATURE SENSOR DEMONSTRATION REPORT (HCMR)

1. BACKGROUND

As a climate change hotspot, the Mediterranean's sea plays a key role in regulating regional climate through sea-atmosphere energy and moisture exchanges—processes closely linked to sea surface temperature and critical to understanding past and future climate impacts (Pastor et al. 2020). The Eastern Mediterranean Sea is also known for being under sampled particularly regarding in situ measurements like temperature, salinity, and currents. This lack of data complicates accurate assessments of trends such as sea surface temperature changes and ecosystem shifts. To address these gaps, satellite remote sensing and reanalysis models are commonly used, but they still require validation through more extensive and frequent direct measurements (Korres et al. 2014). The Calnex PyroMiniBus (PMB201) is a compact, high-performance infrared pyrometer designed for integration into multi-channel temperature sensing systems. Operating within the spectral range of 8 to 14 μm , it can measure temperatures from $-20\text{ }^{\circ}\text{C}$ to $1000\text{ }^{\circ}\text{C}$ with repeatability of $0.5\text{ }^{\circ}\text{C}$. It is used in many industrial and scientific environments where precise, non-contact temperature measurement is required. As part of NAUTILOS Sub-Task 5.3.2, which involves integrating sensors and samplers onto Ferrybox ships of opportunity, the original demonstration platform's infrared sea surface temperature sensor was the POSEIDON-HCMR Ferrybox system. The HCMR Ferrybox system was not operational during the demonstration period, during which the sensor was installed in the HCMR R/V PHILIA. Integration between the sensor and the hosting platform was tested in May 2024, and the T6.1.2 calibration and validation activities were carried out at NIVA's field station and reported in D6.1: Report on the results and methodology of the calibration/validation experiments.

2. DEMONSTRATION PLAN

Demonstration on board R/V PHILIA

- **Specific Objectives**

The goal of this task was to test a new low-cost infrared temperature sensor for sea surface temperature data collection in operational mode and to propose improvements that will enable its widespread adoption by commercial vessels and citizen science initiatives.

The specific technical objectives to meet were

- Testing the sensor and configuration settings involves checking that the measuring system is correctly installed and configured and is functioning as intended.
- Evaluate data acquisition and system functionality. This step assesses the system's ability to reliably collect, store and (if applicable) transmit data.
- Validate the sensor's temperature measurements against reference data from trusted sources, such as a CTD profiler. The aim is to verify the accuracy of the measurements, identify any biases or drifts, and apply calibration corrections as necessary to ensure reliable results.
- Assessing data management, processing and quality control (QC) procedures ensures that the collected data is handled properly from acquisition to final analysis.

- **Platform/equipment involved**

The Research Vessel (R/V) Philia (Fig. 13) and the onboard SeaBird CTD instrumentation were involved in this demonstration. The R/V Philia is a coastal research vessel operated by HCMR, which is based in Heraklion, Crete. Built in 1986, the yacht is 26.1 meters long, has a maximum speed of 10 knots, and can stay at sea for up to ten days. The R/V Philia (https://www.hcmr.gr/en/equipment/researchvessels_underwatervehicles/rvs/) is primarily utilised for marine and coastal scientific research in the Eastern Mediterranean, but it also supports a variety of other tasks such as oceanographic surveys, environmental monitoring, biological sampling, fisheries research, and seabed mapping. It is equipped with advanced navigation systems, sampling gear, and onboard laboratory facilities, making it well-suited for multidisciplinary marine research. The Sea-Bird SBE 19plus V2 SeaCAT Profiler CTD is a high-accuracy instrument designed for measuring conductivity, temperature, and depth (pressure) in both marine and freshwater environments. The temperature sensor of the SBE 19plus CTD has an initial accuracy of ± 0.005 °C and a typical stability of 0.0002 °C per month and it is widely used in oceanographic research, environmental monitoring, and coastal surveys (<https://www.seabird.com/sbe-19plus-v2-seacat-profiler-ctd/product?id=60761421596>)

- **Deployment configuration**

The data acquisition system was designed to continuously log temperature data from a Calex non-contact infrared (IR) temperature sensor that communicates via Modbus RTU over RS232. The setup uses a Modbus-to-RS232 converter to interface the sensor with a Raspberry Pi, which acts as the central processing and data logging unit. The system components are presented below

- Calex IR Sensor (Modbus RTU output) - www.calex.co.uk/product/temperature-measurement/infrared-temperature-sensors/pyrominibus/. The sensor outputs temperature data in Modbus RTU format via RS232/485 port.
- Modbus-to-RS232 Converter. Converts Modbus RTU data from the sensor to RS232/485 protocol, compatible with the Raspberry Pi's USB-to-serial interface or direct UART.
- Raspberry Pi zero-2-w. Functions as the main computer, running Python communicate with the sensor, log data, and perform real-time processing or visualization.
- A lightweight data logging Python script was used to communicate with the Calex PyroMini Bus sensor via Modbus RTU over RS232 using the *minimalmodbus* library. It reads temperature values at fixed intervals, timestamps each reading, and saves the data into a daily CSV file on the local system. The script runs continuously, handles basic errors, and supports remote monitoring via SSH when connected to a mobile network
- Power Supply: The system used a regulated 5 V DC supply for the Raspberry Pi and a separate 12 V supply for the Calex IR sensor. All the power lines are connected to the ship network.
- Positioning system: Position data from the GPS module are time stamped and stored in structured formats on the Pi's storage.



Figure 13: The R/V Philia and the IR sensor installed in the left side mast of the ship.

The Calex PyroMini Bus infrared sensor was installed on the upper open deck mast on the left side of the ship, positioned to directly face the sea surface for accurate temperature measurement (Fig. 13). This location was chosen according to the manufacturer’s guidelines to ensure the sensor only detects infrared radiation from the sea, without interference from ship-related sources such as smoke, fumes, or dust, which could affect the readings. The ship’s CTD system winch is also located on the left side, and the CTD profiler used to validate the sensor's measurements was deployed from the same side, ensuring consistent and directly comparable data from both instruments. To minimize electromagnetic interference (EMI) or signal noise, the sensor was positioned away from motors, generators, and similar electrical equipment. For mechanical installation, the sensor was firmly mounted using two stainless steel brackets, secured with safety nuts and bolts. These brackets allow for adjustment of the sensor’s angle, helping to fine-tune its pitch and roll for accurate targeting of the sea surface.

- **Location**

The sensor was installed onboard the R/V Philia from June 2024 through November 2024. During this interval, the vessel operated for 30 days travelling across the North Aegean, Ionian Sea, and adjacent coastal regions of Greece performing fisheries surveys. A dataset comprising over 250,000 measurements was acquired, covering a cumulative transect distance exceeding 2,000 nautical miles (Fig. 14).

- **Period of occurrence**

The data were collected over two separate periods: from 10 June to 24 July 2024 in the North Aegean, and from 3 September to 13 October 2024 in the Ionian Sea.

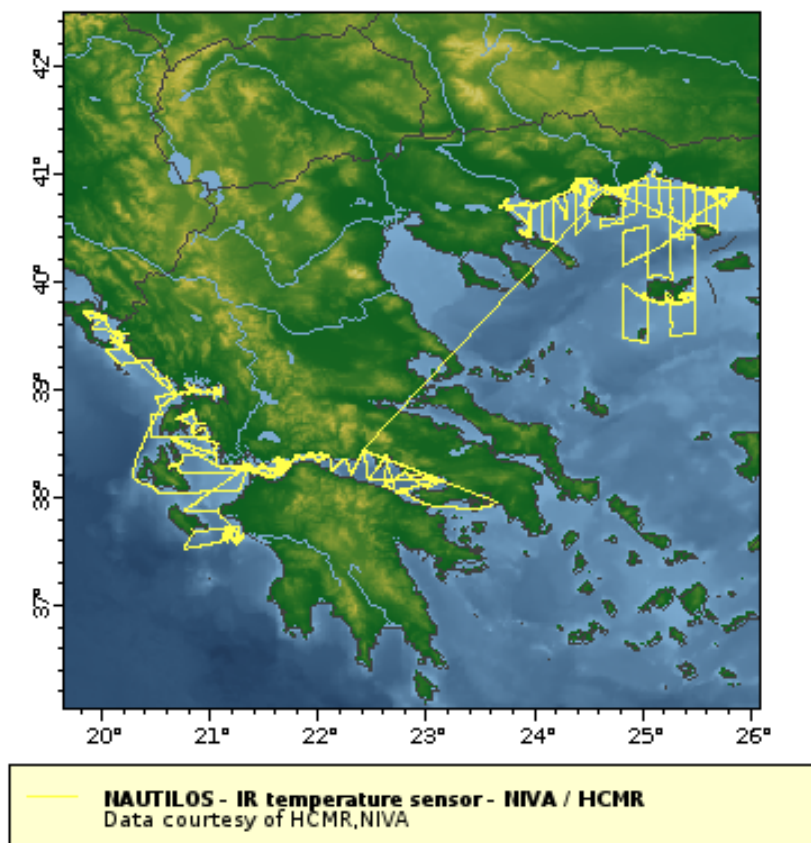


Figure 14: The R/V Philia tracks during the demonstration of the IR sensor.

- **Maintenance, events/issues occurred and actions taken**

The sensor underwent regular maintenance onboard, which involved cleaning the sensor head and removing saline residues. The procedure was straightforward and could be easily performed by the ship’s crew.

- **Data recovery/ Analysis**

The data collected by the Calex PyroMini sensor was stored locally on the system computer (Raspberry Pi), which continuously logs measurements every 10 seconds to a file corresponding to a 24-hour period. A new file is automatically created each day to organise the data chronologically and facilitate later analysis. The system is configured for remote access via a mobile network connection, allowing operators to monitor data in real time or perform system checks during the survey using remote control software. Despite the remote access capabilities, the complete data set is manually retrieved at the end of the survey by accessing the on-board computer and copying the stored data files.

3. RESULTS – COMMENTS – CONCLUSIONS

- **Results**

Operational data must undergo delayed-mode quality control to identify long-term trends and ensure reliability. Whenever possible, sensor data should also be validated against external reference datasets. In the first stage of quality control, the retrieved sensor data were checked and flagged based on the following criteria:

- Minimum Block Length – Detection of incomplete or incorrectly sized data blocks
- Impossible Date – Timestamps that fall outside a valid or expected range
- Impossible Location – GPS coordinates that are clearly erroneous or outside operational zones
- Frozen Date/Location/Speed – Identical values repeated over time, indicating potential sensor or logging failure
- Frozen Temperature (T) – Constant temperature readings over extended periods
- Global/Regional Range (Speed/T) – Values compared against known global or regional climatological limits to detect anomalies
- Gradient and Spikes (T) – Identification of sudden, unrealistic changes or spikes in temperature data

In the second level of quality control, the level 1 QC sensor data were compared with measurements obtained from the SBE CTD operated by scientists onboard the *Philia* during ship-based surveys. A total of 148 CTD casts were processed using the manufacturer’s software, and surface measurements from each cast in the water column were compared against the IR sensor readings (Fig. 15).

All IR temperature values recorded within a ± 15 -minute window of the time of the CTD cast were extracted. The average IR temperature in this window was calculated and compared with the CTD data (Fig. 16).

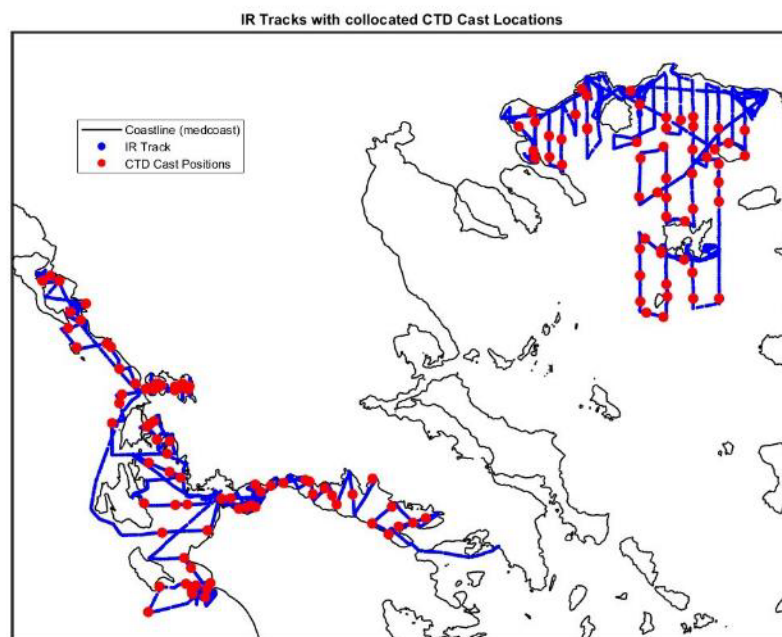


Figure 15: The CTD control points (highlighted in red) for the validation of the IR sensor data.

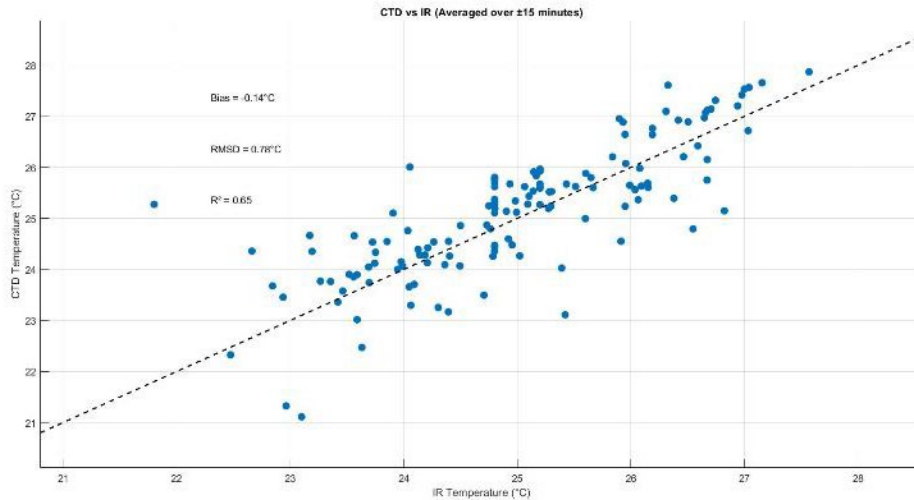


Figure 16: Comparison statistics for IR and CTD temperature.

The Calex IR and in situ temperature sensor measurements were generally in good agreement, considering the expected precision of the Calex IR sensor as specified by the manufacturer). IR sensors measure the true sea surface or "skin" temperature, typically within the top few micrometers of the ocean, while the CTD in situ sensors record temperature slightly deeper, typically averaged over the top 1–2 meters. This difference in measurement depth can result in variations, particularly under conditions influenced by solar heating, wind, or surface cooling, and must be taken into account when comparing datasets for validation or calibration purposes. In addition to this inherent difference between IR and in situ thermistor readings, the Philia demonstration introduced an additional variable: the movement of the ship caused by sea state conditions, which may have affected measurement stability and alignment. The final QC data set of the IR sensor demonstration was uploaded to the NAUTILOS data portal (Fig. 17).

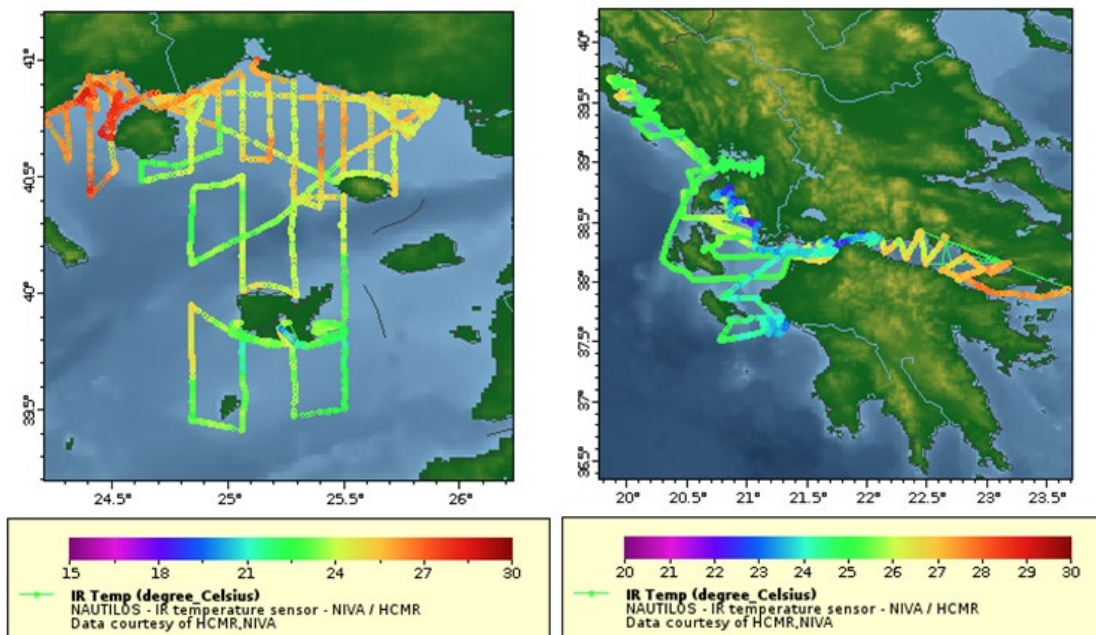


Figure 17: The final dataset visualized in the NAUTILOS data portal.

- **TRL achievement level and project SOP**

The IR temperature sensor for ships of opportunity has been successfully demonstrated under realistic conditions in a relevant operational environment. This low cost and cost-effective technology offers a low initial purchase price (less than 1000 euros, including the sensor and GPS data logger), as well as an open-source configuration that reduces customisation expenses. Its operational costs are minimised due to its low power consumption and robust design, reducing the frequency and complexity of maintenance interventions. This ensures sustained endurance and reliable sensor performance in diverse marine environments over extended deployment periods. Consequently, the Technology Readiness Level (TRL) advanced from 5 (corresponding to the status after WP6) to 7 where a prototype system has been demonstrated in an operational environment.

- **Future plans and Recommendations**

The IR sensor on board the R/V PHILIA will remain active to operate and collect opportunistic data. The NAUTILOS partners who are active partners in the Ferrybox community within EuroGOOS, will collaborate to further develop and optimize the infrared temperature sensor system for integration on commercial vessels following recommendations. To enable reliable, autonomous operational use of the infrared sensing and data logging system on small commercial or fishing vessels, the following technical improvements are recommended:

- **Software & Telemetry:** Enhance the software to support real-time data visualization in cloud infrastructure and remote access via 5G or LTE modems.
- **Power Autonomy:** Integrate solar panels and battery systems to ensure independent operation without relying on vessel power. Power-saving modes should be implemented to extend system uptime during long missions.
- **Sensor Stability:** Mount the sensor on a gyroscopic or gimbal frame to maintain proper orientation toward the sea surface, minimizing the effects of ship movement and improving data quality in rough conditions.
- **Modular Deployment:** Design adaptable mounting hardware that fits a range of vessel types and enables fast installation. Provide user-friendly setup instructions to support use by non-specialist crews.
- **Data Handling:** Develop automatic daily logging and cloud backup systems to secure collected data. Include basic onboard quality control routines and ensure data can be manually recovered at the end of each survey.

IV. SAMPLER FOR PHYTOPLANKTON AND OTHER SUSPENDED MATTER. DEMONSTRATION REPORT (NIVA)

1. BACKGROUND

The sampler for phytoplankton and other suspended matter was developed in Task 3.5 for automated filtration of phytoplankton and EOVs that are conventionally sampled manually using a vacuum filtration setup on a lab bench. The Sampler is based on a McLane Particle and Phytoplankton Sampler (PPS) which is designed for in situ deployment usually attached to moorings. In NAUTILOS, the McLane PPS was disassembled from its deployment frame, and the filter holders, stream select valve, and pump were adapted to a mobile freezer/cooler chest. Additionally, the system was tested and retrofitted for use with ethanol (EtOH) as a preservative for DNA samples. The integration and validation aspects of development were described in Deliverables 5.6 and 6.1. Here, the demonstration of the sampler on the MS Trollfjord Ferrybox in the coastal Norwegian Sea region of the North Atlantic is described in which automated sample filtration for environmental DNA (eDNA) was carried out to assess the sampler performance and DNA quantification from phytoplankton communities. Complementary field demonstrations were also carried out as part of the Horizon 2020 JERICO-S3 project in which the NAUTILOS Sampler was deployed on missions in the Skagerrak on the MS Color Fantasy Ferrybox (Delauney et al. 2024)

2. DEMONSTRATION PLAN

The demonstration was carried out using the MS Trollfjord Ferrybox as an observing and sampling platform. The NAUTILOS Sampler for phytoplankton and other suspended matter was integrated with the MS Trollfjord Ferrybox both in terms of hardware/hydraulic connections and software-based control and collected samples along with complementary Ferrybox sensor observations for other EOVs including salinity, temperature, and chlorophyll a (Chl-a) fluorescence, as well as parallel samples for manual sample filtration (conventional) for ground truthing.

Demonstration on MS Trollfjord Ferrybox

- **Specific Objectives**

The overall aim was to demonstrate the reliability and repeatability of automated filtration using the NAUTILOS Sampler for phytoplankton and other suspended matter, and specifically:

- Assess phytoplankton DNA collection both by automated filtration and groundtruth with manual filtration techniques
- Characterise phytoplankton variability along a large latitudinal gradient with variability in salinity, temperature, and phytoplankton biomass

- **Platform involved**

System was installed in MS Trollfjord Ferrybox.

- **Deployment configuration**

The NAUTILOS Sampler was integrated with the Ferrybox water circulation system as well as the software environment of the Ferrybox. The Ferrybox system pumps water into a series of sensors through a seawater intake valve at ~5 m depth. It is controlled by a custom Labview

program on a Windows-based computer and operates sensors including a Sea-Bird SBE38 inlet temperature sensor, a Sea-Bird SBE45 Thermosalinograph, a Turner Designs C3 optical sensor (Chl a fluorescence, CDOM fluorescence, turbidity), and an ISCO Teledyne bulk seawater autosampler. The NAUTILOS Sampler is a deconstructed McLane PPS system (described in further detail in D3.7, D5.6, and D6.1) that consists of 24 filter holders (47 mm diameter), a central 25-port (filter holders plus neutral port) selection valve, a ceramic gear pump, a water/selection valve, and control electronics. The sampler estimates volume filtered for each sample from the number of pump RPMs during a sampling time period. The sampler was equipped with 0.45 µm PES membrane (Merck Millipore) filters for eDNA sampling. Ferrybox GPS-based location data was used to establish GPS fences to trigger sample collection.

- **Location**

The demonstration using the MS Trollfjord Ferrybox with the Sampler for phytoplankton and other suspended matter was carried out in the southwestern part of the coastal Norway region of the Norwegian Sea (Fig. 18). The transect was in total approximately 700 km in which 19 sampling segments were conducted in roughly equally-sized segments and started 60.8 °N 4.8 °E near Hjeltefjorden, Norway (just north of Bergen, Norway) and ended 69.1 °N 17.7 °E in Ånderdalen/Vangsvik, near Tromsø, Norway.

- **Period of occurrence**

14:53 UTC 1 June 2024 to 03:05 UTC 5 June 2024

- **Maintenance, events/issues occurred and actions taken**

No major maintenance/issues occurred during the demonstration. Several operational issues/bugs were resolved during the calibration/validation activities as part of WP6 and reported in Deliverable 6.1.

- **Data recovery/ Analysis**

Samples collected from the mission were brought back to the lab for processing and analysis. DNA was isolated with the Qiagen PowerSoil kit, according to the manufacturer's protocol, and quantified by NanoDrop. All sensor data and sampling metadata were co-logged with vessel navigation data in 15-minute and 24-hour log files on the vessel, which are automatically transferred over the vessel's satellite communication link to NIVA's onshore FTP server. Data are ingested into NIVA's cloud database for automated quality control and interactive Grafana-based visualisation.

- **Other Relative Activities**

None

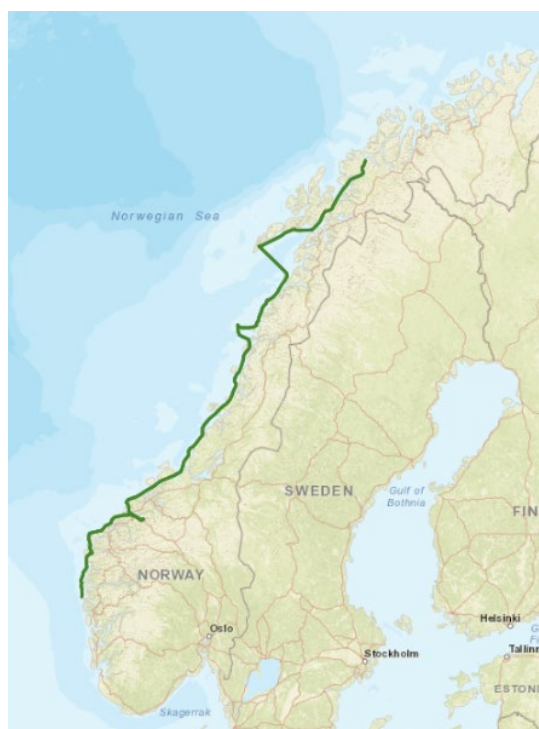


Figure 18: Sampling track for the Sampler for phytoplankton and other suspended matter on MS Trollfjord from Hjeltefjorden to Ånderdalen/Vangsvik, Norway, in which 19 sampling segments were carried out.

3. RESULTS – COMMENTS – CONCLUSIONS

- **Results**

In total, 20 samples were collected in which approximately 2 L was filtered by the NAUTILUS Sampler and a comparison sample was manually filtered using a conventional benchtop vacuum filtration setup. The station number, location, date, time, Chl-a fluorescence, sea surface temperature, and salinity are reported in Table 1. Salinity varied from ~ 16.6 to ~ 32.4 indicating that some regions, especially station TF4 Moldefjorden, had measurable impacts of freshwater from riverine input. Sea surface temperature ranged from ~ 10 to ~ 14.5 °C which is typical for early summer conditions in the region. Chl-a fluorescence was relatively uniform in the sampling region with mean ± 1 standard deviation of 2.1 ± 0.5 mg m⁻³. Comparison of DNA-concentrations recovered from the automated Sampler filtration and manual filtration is shown in Fig. 19. The field-collected samples using the automated Sampler and manually-collected/filtered techniques yielded similar DNA concentrations with median values of ~ 0.8 ng DNA ml⁻¹, although there were some outliers and higher variability in Sampler-collected samples. While the total DNA quantified was not only phytoplankton DNA, the relatively high concentration of ~ 2.1 mg m⁻³ Chl-a fluorescence suggests that phytoplankton DNA comprised a large fraction of the total DNA collected and quantified.

Table 1: Sampling locations and supporting data for the Sampler for phytoplankton and other suspended matter including station number (TF1-19), approximate geographical/coastal region, date, time, longitude (Long), latitude (Lat), Chl-a fluorescence (Chl-a flu), sea surface temperature (Inlet temp), and salinity.

Station number	Geographical location (approx.)	Date (dd.mm.yyy)	Time (hh:mm UTC)	Long (deg E)	Lat (deg N)	Chl-a flu (mg/m ³)	Inlet temp (deg C)	Salinity
TF1	Hjeltefjorden	01.06.2024	14:53	4.781	60.767	2.1	12.1	29.161
TF2	Nord for Sognefjorden	01.06.2024	16:49	4.750	61.136	2.3	13.5	28.715
TF3	Florø	01.06.2024	19:11	4.976	61.566	2.2	12.5	28.768
TF4	Moldefjorden	02.06.2024	05:10	7.293	62.624	2.3	14.5	16.628
TF5	Bud	02.06.2024	14:56	6.869	62.966	1.9	12.9	30.650
TF6	Averøy	02.06.2024	16:16	7.489	63.090	2.0	12.8	29.802
TF7	Trondheimsleia	02.06.2024	19:19	8.875	63.458	2.0	12.9	31.049
TF8	Djupfest	02.06.2024	21:17	9.542	63.766	2.4	12.7	31.728
TF9	Rørvik	03.06.2024	03:44	11.386	64.915	2.5	10.0	32.361
TF10	Brønnøysund 1	03.06.24	06:17	12.043	65.367	2.4	12.5	32.106
TF11	Brønnøysund 2	03.06.2024	07:39	12.156	65.594	1.8	12.2	32.251
TF12	Herøy	03.06.2024	09:30	12.474	65.976	1.9	11.0	29.489
TF13	Træna	03.06.2024	12:44	12.105	66.440	1.9	11.3	31.693
TF14	Ørnes/Glomfjord	03.06.2024	21:20	13.263	66.818	3.0	10.6	32.390
TF15	Bodø	6/4/2023	01:09	14.171	67.240	nd	nd	nd
TF16	Reine	6/4/2023	05:40	13.115	67.930	nd	nd	nd
TF17	Loddingen	6/4/2023	19:40	15.958	68.354	1.2	10.2	32.331
TF18	Harstad	6/4/2023	22:38	16.854	68.805	2.6	10.5	32.262
TF19	Ånderdalen/Vangsvik	6/5/2023	01:05	17.746	69.137	1.2	12.1	29.000

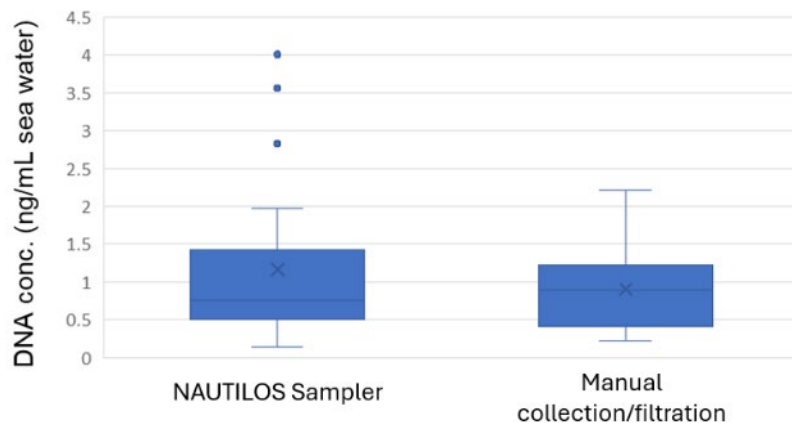


Figure 19: DNA concentrations (ng DNA mL⁻¹ seawater) from samples collected using the automated Sampler (NAUTILOS Sampler, n=19) and manually-collected/filtered samples using a bench top vacuum filtration setup (Manual collection/filtration, n=40).

- **TRL achievement level and project SOP**

The Sampler for phytoplankton and other suspended matter was developed with the goal of autonomous sampling and filtration without user intervention. The Sampler can be deployed on an observing platform (i.e., on a Ferrybox in this demonstration) and automatically start to pump/filter seawater, at a given timepoint or GPS location/fence, through 24 different filter holders, pump samples to dryness, and add EtOH for preservation of DNA. However, the demonstration still involved periodic user attendance to ensure proper operation, so the length of unattended operation beyond 5-6 hours (i.e., 5-6 sample filtration steps) needs to be tested. Based on the level of testing and validation in the demonstration phase, the Sampler for phytoplankton and other suspended matter is at TRL 8, in that the prototype has been successfully demonstrated and qualified with manually-collected/filtered sampling in an operational environment - integrated with an ocean observing platform and autonomously collecting and filtering samples over a reasonable time period for collection of multiple samples in series. Future replicated tests of unattended, autonomous sampling and preserving of samples over a several day time period.

- **Future plans and Recommendations**

The development of an automated sample filtration system in the NAUTILOS project was intended to 1) fill gaps in the measurement of EOVs for which sensor technology does not yet exist, and 2) filter and preserve samples (reagent, cooling/freezing) so that samples can be returned to the lab for analysis. The Sampler has been calibrated and validated for Chl-a and eDNA samples during the project. Future longer-term deployments will be carried out as part of national monitoring programs to collect and preserve Chl-a samples for use with water quality assessments and validation of Chl-a fluorescence data. Additionally, the use of event detection algorithms developed in NAUTILOS will also be investigated for strategic sampling of regions of interest with, for example, high Chl-a or other taxa-specific fluorescence signals, or large changes in temperature or salinity which can suggest a shift to a different water mass or regions of upwelling or strong riverine input.

V. LOW-COST MICROPLASTIC SENSORS BASED ON SELECTIVE NILE RED STAINING AND FLUORESCENCE DETECTION. DEMONSTRATION REPORT (NIVA)

1. BACKGROUND

During the development of the combined sampler and microplastic detection system using the Nile Red staining concept, both the sampler and the detector have been evaluated separately and as a combined unit (D4.4). Integration of the sampler unit with the Ferrybox system on a ship of opportunity was done on the M/S Trollfjord (D5.6). Preliminary data for a large-scale monitoring project along the Norwegian coast have been reported (D9.7).

2. DEMONSTRATION PLAN

Demonstration of microplastic sampler was conducted in M/S Hurtigruten, while the TRL levels of Microplastic detector system (sampler + detector + Ferrybox infrastructure) and Microplastic detector were too low to be evaluated in field conditions and validation can be done in laboratory environment only.

Demonstration of microplastic sampler in M/S Hurtigruten

- **Specific Objectives**

The large volume low cost microplastic sampler consists of a filter holder with filter options from 50-300 μm allowing large sampling volumes (up to 10 000 L) to enable sampling down to background levels (Fig. 20). The sampler unit consists of a closed housing easy to exchange without contact with the surroundings, avoiding sample contamination. The low-cost filters allow taking several samples during a sampling campaign which are shipped back to the laboratory where they are analysed under controlled conditions. The sampler is able to measure the total sampling volumes for samples. Samples ($n=10$) are to be analysed in a special microplastic laboratory with specific equipment (μFTIR , μRAMAN , pyr-GC/MS), number of particles, polymer identification.

The microplastic detection system (sampler + detector + Ferrybox infrastructure) consists of an automatic microplastic sampler, a sample treatment chamber, and an inline particle measurement system (Fig. 21). The large volume sampler uses a mesh filter (50-300 μm) to collect microplastics in the 4-meter surface layer (1000 L to 10 000 L). After transfer to the reaction chamber, the collected plastic particles are treated to remove organic material and stained with a fluorescent dye (Nile Red). Finally, the labelled microplastic particles are moved to the laser detector, where the fluorescence light emission from each particle is recorded. The sampler and laser detector system are designed for operation on 'ships of opportunity' connected to existing infrastructure (Ferrybox) where the microplastic data is acquired in combination metadata (GPS location, timestamps, weather conditions and other sensor data). Measured parameters of the detection system include fluorescent emission intensity of each particle (green and red), total particle counts per sample and total sampling volume. The microplastic detector measures fluorescence labelled microplastic particles in the size range of 1 to 300 μm . It consists of a glass flow channel, a strong blue laser, up to six photodiodes for detection, and electronics coupled to a Raspberry Pi for data recording and processing. Cleaned and stained particles are administered through the glass capillary, where

the laser induced fluorescence emission is recorded from labelled microplastic particles. For each particle, the green and red fluorescent light emission is recorded, processed and stored in flow cytometry data format on the internal memory. Measured parameters for the detector are fluorescent emission intensity of each particle (green and red) and total particle counts per sample.



Figure 20: Installation of the microplastic sampler system on the MS Trollfjord.



Figure 21: The standalone prototype of the combined sampler and oxidation and Nile Red dyeing chamber.

- **Platform involved**

Initial test was performed on the MS ColorLine Fantasy (Oslo-Kiel Ferry) and final installation on the M/S Trollfjord (Norwegian coast Atlantic and polar regions).

- **Deployment configuration**

The sampler unit consisted of a closed housing easy to exchange without contact with the surroundings, avoiding sample contamination. Ten NAUTILOS filter holders were made of stainless steel. The low-cost filters allow taking several samples during a sampling campaign which are shipped back to the laboratory where they are analysed under controlled conditions. A mesh size of 100 µm was used.

- **Location**

Transect lines are drawn schematic, not showing the exact route of the ship (Fig. 22). Codes and transect names of Ferrybox sampling for analysis of microplastics in 2023 are given in Table 2.

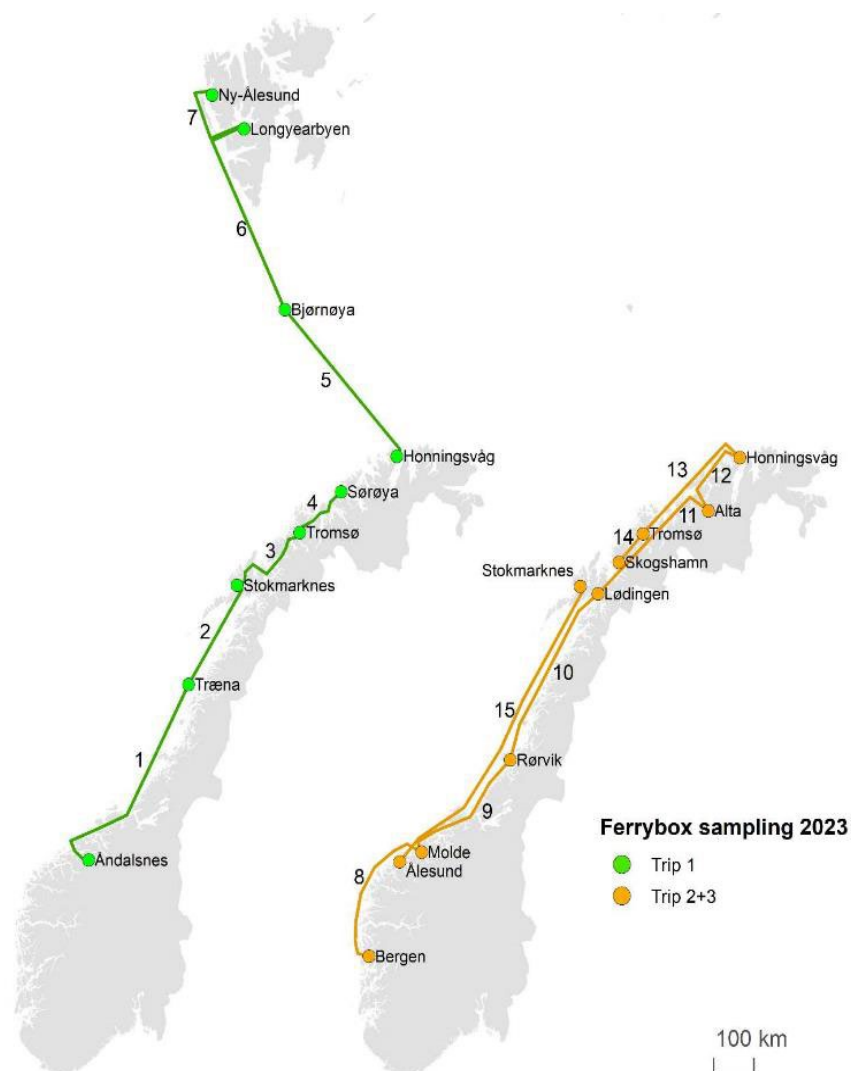


Figure 22: Transects for the analysis of microplastics in Ferrybox samples in 2023.

Table 2: Detailed information on the 15 transect sampled during the 2023 sampling campaign on the MS Trollfjord.

Nr.	Trip	Transect	Nr.	Trip	Transect
1	1	Åndalsnes-Træna	8	2+3	Bergen-Molde
2	1	Træna-Stokmarknes	9	2+3	Molde-Rørvik
3	1	Stokmarknes-Tromsø	10	2+3	Rørvik-Lødingen
4	1	Tromsø-Sørøya	11	2+3	Lødingen-Alta
5	1	Honningsvåg-Bjørnøya	12	2+3	Alta-Honningsvåg
6	1	Bjørnøya-Longyearbyen	13	2+3	Honningsvåg-Tromsø
7	1	Longyearbyen-Ny-Ålesund	14	2+3	Tromsø-Skogshamn
			15	3	Stokmarknes-Ålesund

- **Period of occurrence**

Microplastics were sampled at three cruises with Hurtigruten ferries in 2023 with a filter system with a 100 µm mesh size, at a depth of approximately 4-5 m. First cruise between Åndalsnes and Ny-Ålesund (September 11.-17.), second cruise between Bergen and Skogshamn (October 21.-27.) and third cruise between Bergen and Ålesund (December 8.-15.).

- **Maintenance, events/issues occurred and actions taken**

Not applicable

- **Data recovery/ Analysis**

The samples were analysed in NIVAs specialised microplastic lab in batches of 7-8 samples including 1-2 field blanks samples where the number of the different microplastic (fibres or fragments) and polymer composition was determined after sample preparation including oxidation and filtration before µFTIR analysis. The microplastic data was then combined with the meta Ferrybox data of the different transects.

- **Other Relative Activities**

Metadata was acquired with the Ferrybox system installed on the MS Trollfjord, the sampling system was stopped and started on-line through the Ferrybox.

3. RESULTS – COMMENTS – CONCLUSIONS

- **Results**

During the initial cruise, microplastic (MP) levels ranged from 0.05 MP m⁻³ to 0.8 MP m⁻³, however, several results were below LOD and most of the results were below LOQ, and caution is advised when interpreting both the patterns and precise levels. The open waters between mainland Norway and Svalbard recorded the lowest levels. Only a few of the samples collected across three cruises showed elevated microplastic levels, indicating that there is little microplastic over 100 µm in these marine areas. Nonetheless, these levels were significantly lower than those found in the inner Oslofjord for particles sized between 100 µm and 5 mm. The sample collected along the transect between Tromsø and Sørøya showed the highest levels, also marking the peak level among all Ferrybox samples from the 2023 sampling.

- **TRL achievement level and project SOP**

The integration of both systems revealed problems in going from large volumes and flows ($L \text{ min}^{-1}$) to micro volumes and flows ($\mu\text{l min}^{-1}$), and the TRL of the completed system stayed at TRL 3, the detector system reached TRL 4, whereas the low cost sampler reached TRL 7 and was demonstrated at the relevant environment and installed on the M/S Trollfjord and connected to the existing Ferrybox on board. This sampling system was successfully used for the Norwegian microplastic monitoring program along the Norwegian coast and Svalbard by the Norwegian Environment Agency.

- **Future plans and Recommendations**

The NAUTILOS low cost microplastic sampler allows continuous sampling and monitoring of MPs in the marine environment. The sampling module can be installed as an add on of Ferrybox systems and used in combination with microplastic analysis in specialised laboratories and equipment μFTIR , μRAMAN or pyr-GC/MS. The samplers are easy to replace and changed by the ship's crew. Another advantage of the samplers is that they are completely closed to avoid sample contamination allowing accurate and low-cost sampling of microplastics.

VI. CARBONATE SYSTEM/OCEAN ACIDIFICATION SENSOR. DEMONSTRATION REPORT (SYKE, NIVA)

1. BACKGROUND

The carbonate chemistry sensor used in the Ferrybox demonstration includes an Endress+Hauser ISFET (ion-sensitive field-effect transistor) pH sensor. This sensor is commercially available for laboratory and industrial applications and was improved for flowthrough application using a custom build flowthrough cap. The flowcap construction is given in D5.6., and standard stock of PVC parts were used to keep the costs low. The housing was pressure tested (at 1.5 bar) and noted suitable to be integrated in Ferrybox systems. In the tests, a simple M12-USB A serial connection was noted suitable for data transmission from the sensor to a computer.

The typical pH-sensors used previously in Ferrybox applications include glass electrodes and spectrophotometric devices, but also ISFET sensors have been used. Glass electrodes require frequent calibration and are not considered as relevant for climatic studies where high accuracy and high precision is needed. Spectrophotometric devices, with higher precision and accuracy, are rather expensive and sometimes complicated to use (Okazaki et al. 2017). Some ISFET sensors are rather inexpensive, like the one tested here, but there is limited amount of information on their suitability for oceanic observations.

The tested sensor was Endress+Hauser Memosens CPS77E ISFET pH sensor with an integrated Pt1000 temperature sensor for temperature compensation. According to the manufacturer, it has a response time (90%) $t < 5$ seconds, repeatability ± 0.01 pH, and average error 0.02 pH over range of pH 1 to pH 13, at 25°C. The laboratory tests in WP6 noted that the Endress+Hauser ISFET pH sensor has a mean absolute error 0.023 pH units, which makes it not suitable for “climate” studies. Such uncertainty is acceptable, however, for “weather” level studies, and for citizen science applications.

Other NAUTILOS carbonate system sensor developments, including pCO₂ sensor and another pH sensor, have been tested in Task 7.1, in aquaculture applications. These are reported in D7.2.

2. DEMONSTRATION PLAN

Demonstration on Ferrybox system in Baltic Sea (Syke)

- **Specific Objectives**

In this demonstration we tested how the pH sensor works in very dynamic coastal waters in the Baltic Sea, where the carbonate system is largely driven by biological activity and pH is varying a lot (Honkanen 2024). Our specific aims were to detect long-term durability and drift of the sensor. As pH in brackish waters is very dynamic, pH is rather complicated to measure accurately in field conditions (given the sensors are in commercial ferry) and different methods are measuring pH at different scales, the actual field validation is complicated. We opted to compare our test sensor with a commercially available spectrophotometric method, with an instrument attached to the flowthrough system and follow the sensor performance against commercially available buffer solutions. As the carbonate system dynamics vary largely between seasons and the water temperature changes drastically, we considered that

the demonstration needs to cover the full annual cycle, to evaluate if these affect the sensor performance.

- **Platform involved**

Two Endress+Hauser Memosens CPS77E ISFET pH sensors were deployed on an existing ferrybox system operated by Syke on a commercial cargo ship m/s Finnmaid (itameri.fi/en/the-baltic-sea-now/automatic-observations-from-ships/), travelling between Helsinki (FI) and Travemünde (DE). The existing Ferrybox instrumentation consisted of Chl-a fluorometer/turbiditymeter (Wetlabs FLNTU), Phycocyanin fluorometer (Trios MicroFlu-Blue), CDOM fluorometer (Trios MicroFlu-CDOM) and a thermosalinograph (Seabird SBE45). In addition, the Leibniz Institute for Baltic Sea Research Warnemünde (IOW) is operating a system for measuring trace gases on the ferry (www.io-warnemuende.de/finnmaid_en.html).

- **Deployment configuration**

Ferrybox water inlet is at nominal depth of 5 m. There is a constant sample water flow of ca. 3.5 l/min through all Ferrybox sensors during transit, while for duration of harbour calls the water is automatically replaced with a dilute cleaning solution. For most of the sensors the measurements are taken every 20 s.

For connecting the pH sensors in-line with the system, custom PVC cuvettes were built using standard PVC pipe parts and 3D -printed thread adapters (Fig. 23). Using the rotatable terminal head, the sensor is installed into the cuvette with its sensor head in a 30' to 45' angle with the flow, as recommended by the operating manual.



Figure 23: Left: The custom cuvette and the sensor. Right: The sensors connected in series with the Ferrybox instruments. Photos Sami Kielosto.

- **Location**

The distance between Helsinki (FI) and Travemünde (DE) is about 1200 km, along the ship's transect. Ferry transects follow the same track and the route typically goes east of the Gotland Island (Fig. 24), but occasionally also western passages take place. In this study, we analyse the data using latitudes as a spatial dimension.

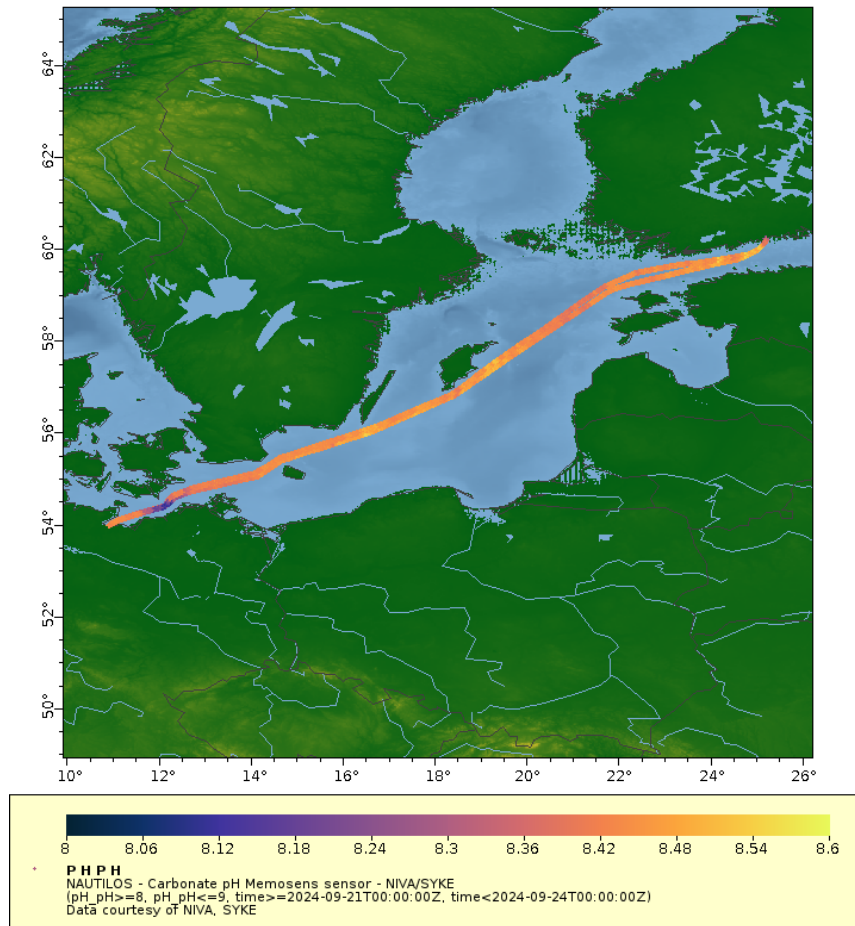


Figure 24: Typical cruise track of ferry Finnmaid, including pH measurements presented in colour scale.

- **Period of occurrence**

Two Endress+Hauser Memosens CPS77E ISFET pH sensors were deployed on an existing Ferrybox system on m/s Finnmaid, from January 2024 and November 2024 to March 2025. The transect between Helsinki and Travemünde lasts approximately 30 hours, while ships stay in harbour for unloading/loading of cargo for 6-7 hours.

The deployment was split in two phases. In the first phase, from January to November 2024, a single pH sensor received from NIVA was used. Accurate pH reference data for this period was received from IOW. The second phase started in November 2024 when a new but otherwise identical sensor was installed in series with the first sensor, in order to observe any differences between the sensors. During this phase pH buffers of 4.01, 7.00 and 9.00 pH were measured every two weeks to keep track of the sensor drift and to evaluate the feasibility of bi-weekly calibration.

- **Maintenance, events/issues occurred and actions taken**

Calibration: For the first test (Jan 2024 - Oct 2024) build in calibration of Memosens sensor was used and using commercial buffers (pH 4.01 and 7.00) we noted that it was slightly off in March 2024 (readings being 4.14 and 7.12-7.13) and remained practically similar until Oct 2024 (readings being 4.15 and 7.17). In Oct 2024 both sensors were calibrated using 2-point calibration (4.01 and 7.00) using their Bluetooth interface. However, on later occasions we could not get the Bluetooth connection to work anymore on either of the sensors and were

left with no means to re-calibrate them on run. Instead, we periodically measured pH buffers of 4.01, 7.00 and 9.00 to track the drift of the sensors.

Periodic maintenance: The Memosens pH sensors were inspected and cleaned every two weeks. There was no visible growth on the sensor, so only tap water was gently sprayed on the element to clean it.

Issue 1: Unreliability of the USB data connection in an industrial environment. On the ship both sensors were connected to a data logging laptop, each via a separate USB adapter cable and a 10m long USB extension cable. Almost on a weekly basis the connection to either of the sensors would be randomly lost in a way that would require the sensor's USB cable to be disconnected temporarily before the connection could be re-established. We assume this issue was due to electrical interference, as it became very rare once we reorganized the 230V supply wiring for our control and instrument cabinets. This issue caused most of the gaps in the data, proving once again that USB is not as robust for field instrumentation as one would hope.

Issue 2: Inadequate durability of the 3D printed cuvette part. Our original cuvette design was flawed in a way that stressed the 3D printed sensor adapter causing it to eventually break. This was successfully solved by using a clamping structure that presses the adapter instead of stretching it. This will also allow the only 3D printed part of the design to be replaced with a cheap commercially available part.

Issue 3: Permanent loss of access to sensor's calibration function. Initially the calibration function of the sensor could be accessed either directly via its user interface or via its Bluetooth application. However, after the first calibration of the sensors, the calibration function disappeared from the user interface, and the Bluetooth connection could not be established anymore. We did not contact the customer support about this issue but continued to follow sensor drift using buffer solutions (which may be even less prone to errors than if the sensor had been several times re-calibrated on board the ship, and allows for the determination of long-term drift).

- **Data recovery/ Analysis**

Memosens pH data was logged with a separate computer, using M12-USB A serial connection. It would have been possible to connect the sensor to the main Ferrybox computer, but this was not seen as necessary during the test period.

Two data files are generated daily, using python-scripts, at the end of the day. UTC time is used both for data and generating file names:

- DELAYED_ferrybox-finnmaid_ph_YYYYMMDDhhmmss.txt for daily pH and temperature data from logger files as received from the sensor.
- DELAYED_ferrybox-finnmaid_location_YYYYMMDDhhmmss.txt for daily Ferrybox data extracting time, location and flow rate data from main Ferrybox data.

If both files were available for a given day, the data were sent to Nautilus FTP server.

Data were analysed against auxiliary IOW spectrophotometric pH analysis (see below), Memosens pH sensor is matched with IOW data by merging on nearest neighbor with 3 s maximum difference. Typical Finnmaid ferry transect contains approximately 500-600 pH data points when using IOW spectrophotometric system (3 min intervals) and approximately

10000-11000 data points when using Memosens sensor (10 sec intervals). Data coverage is roughly 75%, as the connection issues hindered data collection especially in the spring 2024.

- **Other Relative Activities**

In the ship, we used Furuno GP-33 digital GPS receiver for locations. Ultrasonic flow meter (Cynergy3 UF25B, with accuracy 5%) was used to flag pH measurements invalid if flow is less than 3 L min⁻¹.

We received pH data for comparison from the Leibniz Institute for Baltic Sea Research Warnemünde (IOW), who has a Contros HydroFIA pH in the same flow-through system as the tested Memosens pH sensor. Contros is measuring pH using spectrophotometry and m-Cresol purple dye (Aßmann et al 2011). Contros pH was pre-processed, and quality-flagged by IOW.

3. RESULTS – COMMENTS – CONCLUSIONS

- **Results**

The annual pH variability in the transect is shown in Fig. 25. In early spring, pH is low, as pCO₂ has accumulated in the surface waters (Honkanen et al 2024) and primary production is very low. Spring bloom starts in March, in the southern part of the study area, pCO₂ starts to decline and pH to rise. In the northern part of the study area, the spring bloom starts in April-May. Cyanobacteria blooms take place in June-August, especially in the northern part of the study area and consequently pH is having the highest values at that period. After September, thermocline breaks down, and the pCO₂-rich and low pH deeper waters are introduced to the surface. High bacterial demineralisation of organic matter, coinciding with decreased primary production, keeps the pH low. Overall, in the Baltic Sea, the annual variation in pH is from 7.5 to 9.2 pH units, thus much larger than in the open ocean.

Fig. 26 illustrates one of the transects (30.4.-1.5.2024) showing the high basin wide variability of pH, mainly driven by spring phytoplankton bloom intensity. The difference between sensor readings is approximately 0.4 pH units, Contros showing lower values. The higher noise of Memosens sensor is especially visible when zooming in a smaller section of the transect (insert in the figure). While passing this very dynamic area, shown in the insert, it is noteworthy that both sensors seem to respond similarly to pH fronts in the area, as the initial drop in pH and the follow-up peak are similarly reproduced by both sensors.

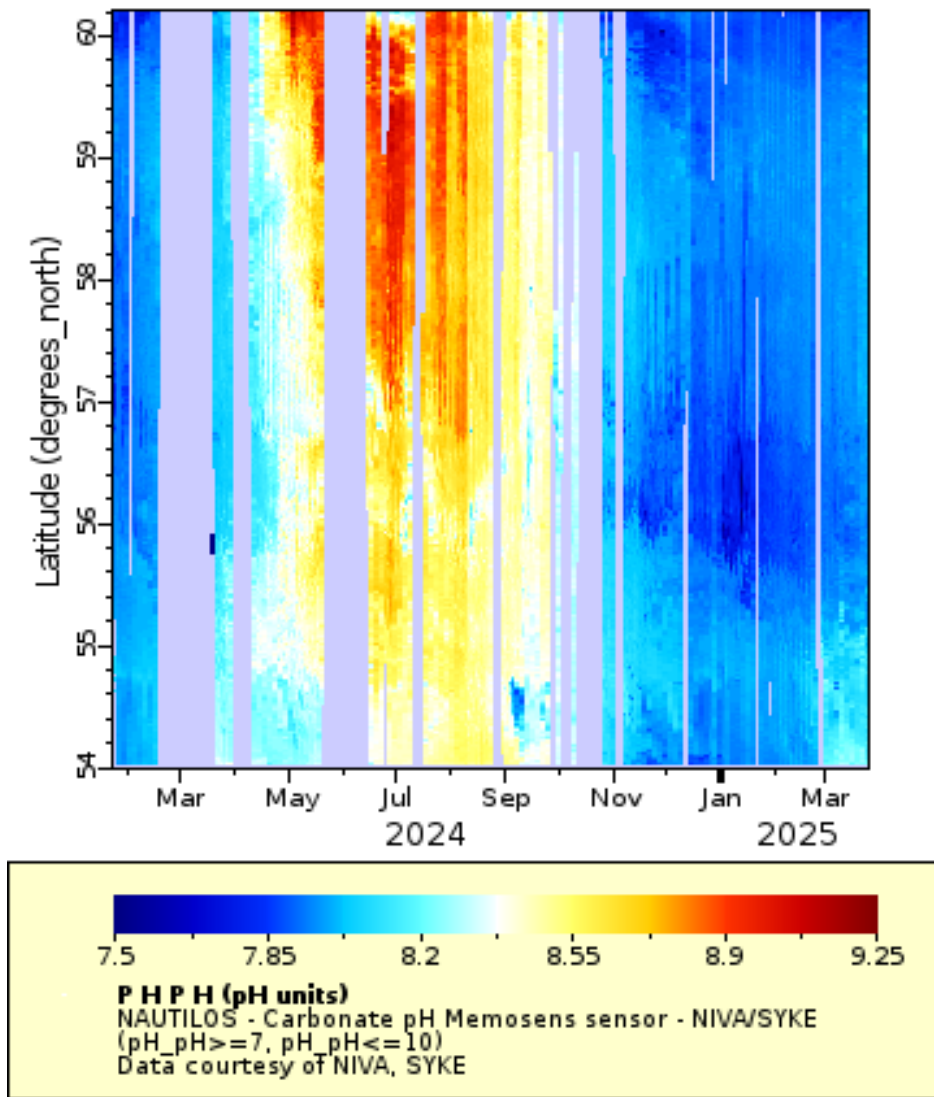


Figure 25: Spatiotemporal development of pH in the Baltic Sea from winter 2024 to spring 2025. Data is measured with Endress+Hauser Memosens CPS77E ISFET pH sensor installed onboard ferry Finnmaid. Refer to Fig. 21 for the location of the ship between Helsinki (north) and Travemünde (south). Grey area in the plot indicates when measurements have not been available.

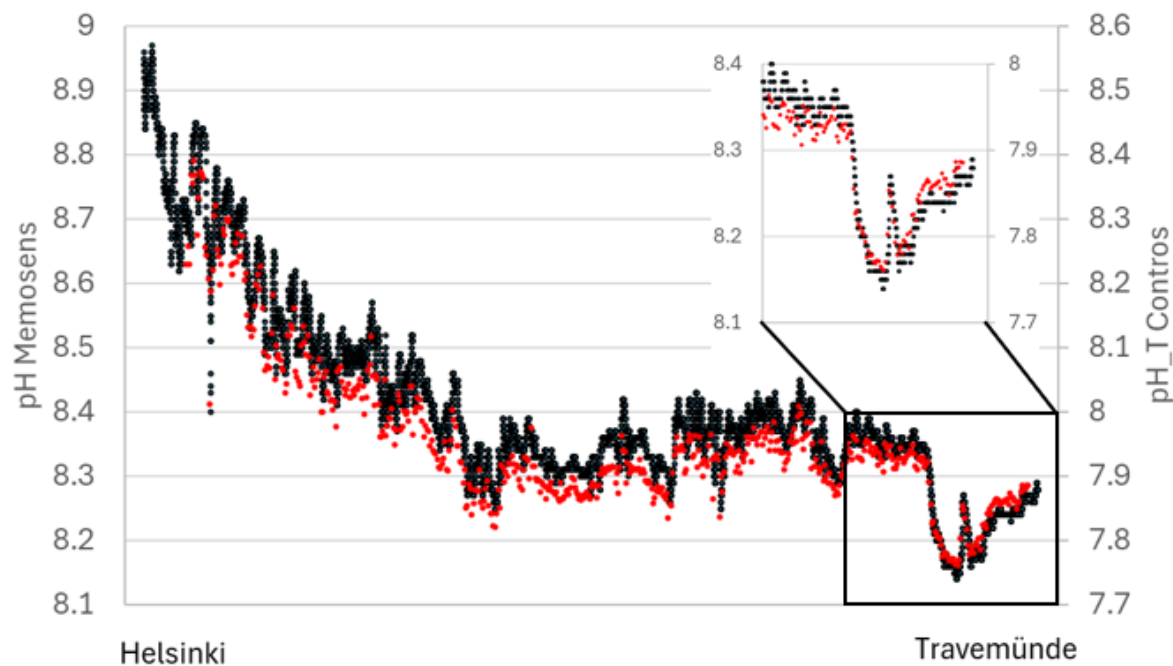


Figure 26: One transect between Helsinki and Travemünde (on 30.4.-1.5.2024) illustrating the large basin-wide variability of pH and how Endress+Hauser Memosens CPS77E ISFET pH sensor (black) and Contros HydroFIA (red) disagree with the measurement scales, but agree with range of variability. The insert in the right upper corner zooms in the southernmost part of the transect and illustrates how sensors read similarly the small-scale variations in pH.

Overall, the two different types of pH sensors showed very similar trends throughout the test period (Fig. 27). The offset between sensors was consistent and around 0.4 pH units. As we know from the calibration error of Memosens, for this period, it showed values 7.12–7.17 pH units for a buffer solution with pH 7.00. Though both sensors used a reference temperature of 25°C., there was a slight temperature dependency of the difference (Fig. 28), but it could also be related to the drift of Memosens calibration throughout the measuring period (Fig. 29) (and at the period the water temperature rose). The remaining difference (approximately 0.25 pH units) is likely due to the difference in measuring principle and shortage of not making Memosens calibration using buffers in brackish water (which were not available) (Müller et al 2018). McLaughlin et al (2017) showed that while ISFET and spectrophotometric pH values generally agreed well, with average difference of 0.005 pH units, in some cases the difference was about 0.2 pH units.

Therefore, a more robust examination of Memosens calibration for brackish water application is required. However, the trends with ISFET and spectrophotometric sensors were very similar, and the results can be used interchangeably once the Memosens data is validated against spectrophotometric ones.

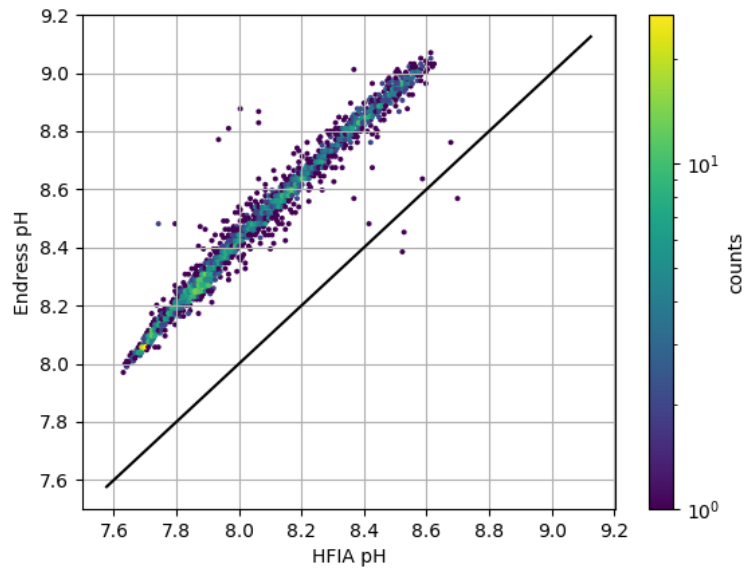


Figure 27: Relationship between Endress+Hauser Memosens CPS77E ISFET pH sensor and Contros HydroFIA pH sensor measurements. Black line is 1:1 fit. For the whole range, the difference is approximately 0.4 pH units.

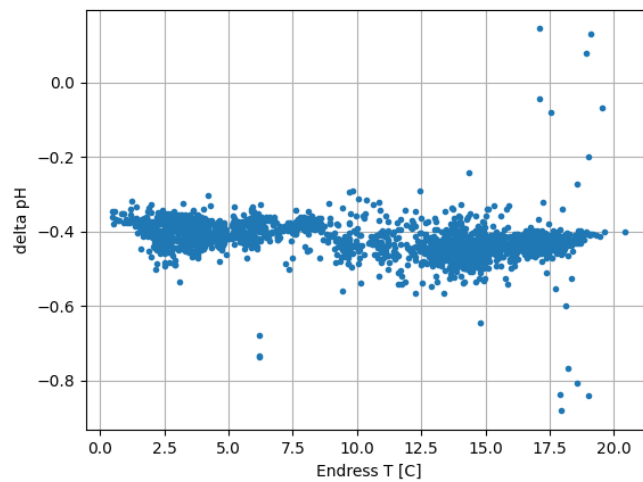


Figure 28: The difference between Endress+Hauser Memosens CPS77E ISFET pH sensor and Contros HydroFIA pH sensor measurements against water temperature, showing a slight increase of difference as water warms up (see also Fig. 29, as this may have been related to the sensor drift as function of time).

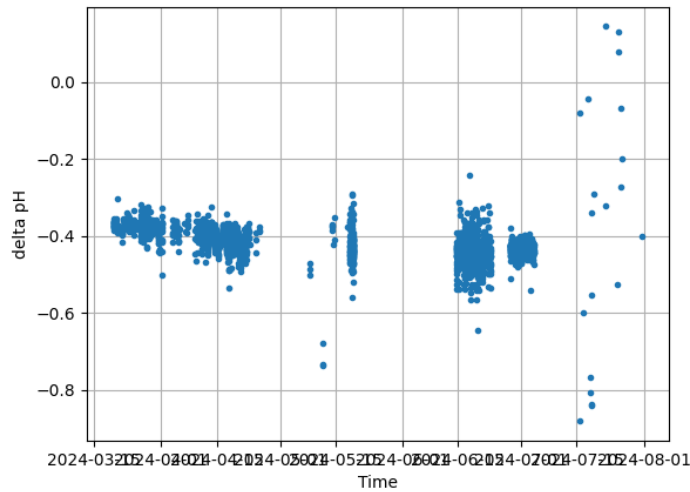


Figure 29: The difference between Endress+Hauser Memosens CPS77E ISFET pH sensor and Contros HydroFIA pH sensor measurements against the date (from March 2024 to August 2024) showing a slight increase of difference possibly related to sensor drift.

In a second period of demonstrations, October 2024 onwards, we used a Memosens sensors with fresh calibration using commercial buffers (4.01 and 7.00) and followed the sensor drift during maintenance visits to the ferry, by measuring the buffers 4.01, 7.00 and 9.00 pH units (Fig. 30). The visits were done from December to late March, approximately at two-week intervals. On average, the shift during two weeks was 0.041 and 0.037 pH units when using buffer solutions 7.00 and 9.00, respectively. The largest shift within two-week periods was 0.1-0.15 pH units. Overall, during the period of three months the cumulative drift was 0.07 pH units at pH 7 and 0.02 pH units at pH 9.00. The absolute error of the sensor is about 0.023 pH units (as determined in WP6) and the observed drift (between two-week measuring points) is even larger.

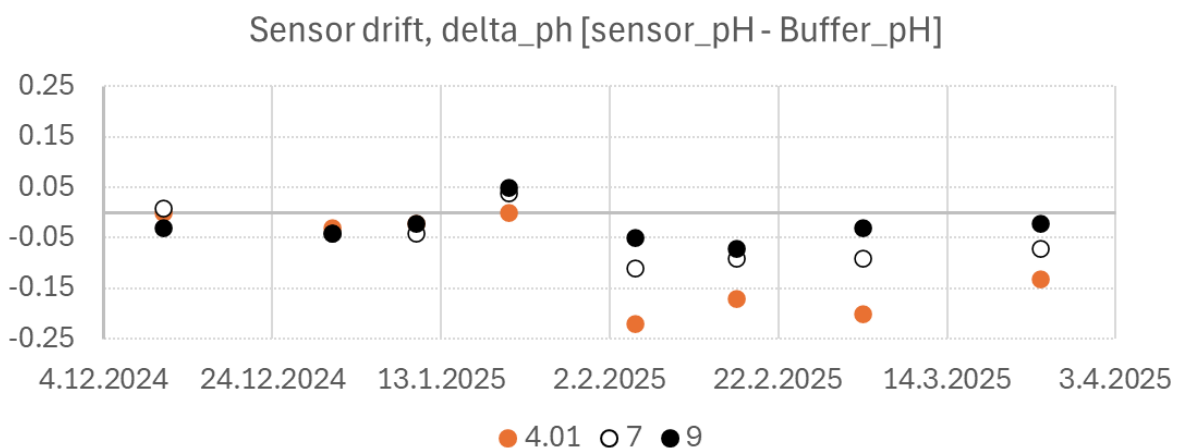


Figure 30: Drift of Endress+Hauser Memosens CPS77E ISFET pH sensor installed in ferry Finnmaid. Sensor was calibrated 21.10.2024 and calibration was followed using buffer solutions.

- **TRL achievement level and project SOP**

As the Memosens sensor itself is already a commercial one (TRL 9) for various uses, the TRL levels used in the context of NAUTILOS project refer to its usability for operational oceanographic observations. After solving issues for flow-through measurements (WP5) and laboratory calibration (WP6), Memosens pH sensor was considered to be at TRL level 5-6 for such activities. In this work we demonstrated that the sensor works in operational oceanographic settings, raising the TRL level to 7-8. Part of the remaining issues with sensor operations (related to USB connections) were partly solved during the demonstration, but the loss of functionalities during the missions (like loss of bluetooth connection and calibration function) call for further tests prior to TRL level is at 9. Issues with calibration offset (difference between Memosens and Contros sensors) are not related to the Memosens sensor itself, but to the difficulty in performing high quality pH validation measurements in low saline environments. Memosens followed closely the performance of top-class spectrophotometric Contros pH sensor (with price difference of approximately 30x), but with lower precision, as known for these technologies. It also clearly needs frequent calibration, which again is technology dependent and not an issue which lowers TRL level. To conclude, we consider that during NAUTILOS the TRL level of Memosens for oceanographic observations has been raised up to 7-8, and TRL 9 should be easily achievable once issues with connection failures and calibration are solved.

Other T4.1 sensors included in WP7 demonstrations (ST7.1.2 Aquaculture Observing Systems) and presented in Deliverable 7.2 include the Durafet pH sensor and pCO₂ sensor. The highest TRL achieved for the Durafet pH sensor was TRL 5 due to a grounding issue that occurred in the demonstration environment (but was not occurring during other in situ testing in WP6), possibly linked to power supply issues at the offshore fish farm. The pCO₂ sensor achieved a TRL level 9 after the demonstration at the fish aquaculture farm where data was collected for a ~1 month period. Overall, for the T4.1 Carbonate system sensors, the TRL achieved by the pH sensors in the context of NAUTILOS was 5-8, and the highest TRL achieved was TRL 9 (pCO₂ sensor).

- **Future plans and Recommendations**

Although the Memosens sensor does not have the accuracy needed for climate studies, the wide variation in pH observed in the Baltic Sea (from 7.6 to 9.2, using Memosens measurements) is so great that main features can be easily covered with such low-cost sensors. Accurate (and expensive) measuring devices for measuring pH are only available in quite a few places. If the validation and maintenance of the measurements of cheaper devices can be made to work, they can complement accurate measurements efficiently, e.g. as citizen science sensors.

SYKE is now testing the Memosens ISFET sensor more, after the NAUTILOS project, and using it in our research vessel, to be compared with additional pH measurements. The next step in the Baltic Sea monitoring community (Finland, Sweden, Estonia, Germany and Poland involved) is to exchange experiences in using various sensors for carbonate system variables, to guide sensor selection for national monitoring programs, and inform the proper sensor calibration protocols. The issues encountered with the ISFET technology will be presented during these gatherings.

VII. FERRYBOX STREAM DATA ANALYSIS DEMONSTRATION REPORT (DFKI)

1. BACKGROUND

NIVA provided an annotated dataset recorded with the Ferrybox deployed on the MS Color Fantasy (cf. Section II), which covers 2023-03-01 until 2024-10-31. The dataset contains 124 algal bloom events identified based on Chl-a primarily with respect to O_2 , salinity and CDOM as well. The tested data analysis software includes concept drift detection algorithms implemented by DFKI (cf. D4.6 and D7.2). The event detection is extended by machine learning methods provided as part of the open-source library *sklearn*, which provides supervised learning approaches. We further build upon the multi-objective optimization library *optuna* to efficiently identify the most promising model configurations.

2. DEMONSTRATION PLAN

Demonstration on annotated data from MS Color Fantasy

- **Specific Objectives**

In this demonstration we show real-time event detection capabilities of a data analysis software system on an annotated data set containing potential algal bloom events. We compare different approaches and evaluate them in terms of Precision (ratio of detected events being relevant) and Recall (ratio of relevant events detected). As this demonstration is not concerned with achieving a specific result, we instead provide a Pareto front plot of various candidates with different ratios of false positives and false negatives to gain general insight into the potential of real-time algal bloom event detection.

- **Platform involved**

Ferrybox on MS Color Fantasy deployed by NIVA as described in Section II.2 in this deliverable.

- **Deployment configuration**

For the configuration of the Ferrybox, cf. Section II.2, information concerning MS Color Fantasy.

The data set is split in three partitions, training (2023-03-01T00:00 until 2024-03-02T06:00), validation (2024-03-02T06:01 until 2024-05-16T06:00) and test (2024-05-16T06:01 until 2024-10-31T23:59) to ensure a similar number of events in each partition. The data are cleaned as per the operator's guidelines; if system pump information is available, only data with an active system pump are used. Port times are removed by checking for the system pump flag and the ship's speed. In case of missing data in individual sensors, missing values are front-filled, i.e. the last known value is repeated until new measurements are available. If a row is missing measurements from all sensors, it is dropped instead.

Training and validation of the models are conducted under real conditions, so training data is older than validation and test data. The models are fitted solely on the training data, so validation results depend on the generalization capabilities of the models and the quality of the data set, i.e. is the training data representative of the entire data set.

We use *optuna* to optimize over the course of 4000 trials. Initial tests with a larger number of trials have shown marginal improvement after approximately 3500 trials.

Configuration parameters include:

- Normalization of the data set: None, or standardization based on the training data
- Feature selection: Chl-a is always included, all other parameters can be toggled on or off
- Feature engineering:
 - Size of the sliding window: 4 to 20 minutes of data
 - Manipulation: None, mean of the sliding window, standard deviation of the sliding window, or mean and standard of the sliding window
 - Maximum number of repetitions for missing value imputation: 1 to 1000 (log scaling)
- Models and their hyperparameters
 - AdaBoost
 - Number of estimators: 10 to 200 (log scaling)
 - Learning rate: 0.1 to 20.0 (log scaling)
 - KNN
 - Number of neighbors: 3 to 21
 - Random Forest
 - Number of estimators: 10 to 200 (log scaling)
 - Max depth: 2 to 24 (log scaling)
 - Neural Network
 - Epochs: 10
 - Batch size: 32
 - Number of layers: 1 to 6
 - Number of neurons per layer: 4 to 128
 - Dropout probability: 0.1 to 0.5
 - Optimizer: Adam, or SGD

- **Location**

See Section II.2, information concerning MS Color Fantasy.

- **Period of occurrence**

NIVA provided data with annotated events of suspected algal blooms from 2023-03-01 until 2024-10-31. Analysis was conducted afterwards in the lab.

- **Maintenance, events/issues occurred and actions taken**

Not applicable (software)

- **Data recovery/ Analysis**

The dataset contains 124 annotated events. The majority of these events occurred in May and June 2024 in Oslofjord and Skagerrak (Fig. 31).

The domain experts annotated 30 events in 2023 and 94 events in 2024. An intuitive split of the data set would be partitions that are equal in size such as 2023 for training and 2024 for test, however the uneven distribution of annotated events might impact results, if too few representative events are available for training. Similarly, the imbalance in event locations might impact predictions in Kattegat and Kiel Bay. However, the current split has a higher ratio of events to non-event data in the validation and test set.

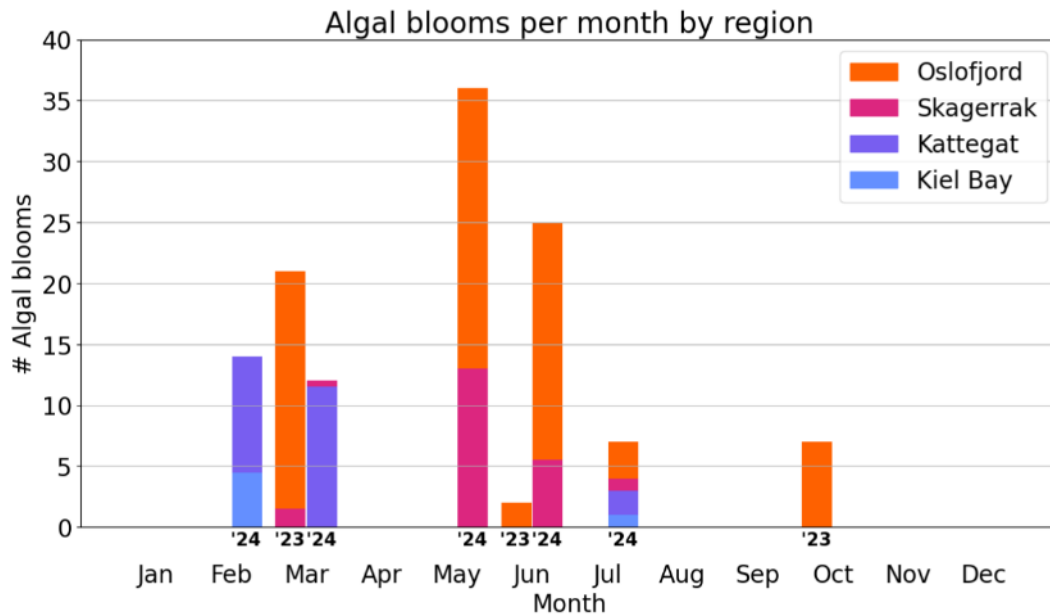


Figure 31: Spatiotemporal distribution of the annotated algal bloom events.

- **Other Relative Activities**

None to report

3. RESULTS – COMMENTS – CONCLUSIONS

- **Results**

Some of the best candidates for the event detection as per above Pareto front achieve Precision-Recall scores of (0.7, 0.76), (0.77, 0.64), (0.86, 0.5), (0.9, 0.42) (see Fig. 32). These particular models might be promising predictors for use with a sampling strategy in the future, as the number of falsely predicted events is on the lower end with 30% to 10% false positives respectively. A high precision means a low number of false positives. Hence, the best candidates might provide a good starting point for further scientific experiments and analysis of water samples in the lab in future work. However, they are not suitable as warning systems yet due to a larger number of false negatives, warnings of algal blooms may often be correct, but many algal blooms would be missed.

We computed fANOVA feature importance scores to determine the most important sensors in the event detection. The most important parameters are CDOM and CO₂ with scores of 0.42 and 0.26 respectively, all other parameters were assigned scores below 0.08, with all scores summing to 1. Chl-a was always included and could therefore not be assessed using this method. This result indicates that CDOM and CO₂ sensors might be more important than others, although achieving better event detection results might yield new insights.

Concept drift detection approaches proposed in D4.6 and D7.2 failed to achieve meaningful results, with the best models achieving Precision-Recall scores of (0.001, 0.95) to (0.1, 0.4). Concept drift detection results show a strong bias in favour of high recall with low precision, meaning that the detectors trigger too often resulting in a very large number of false negatives.

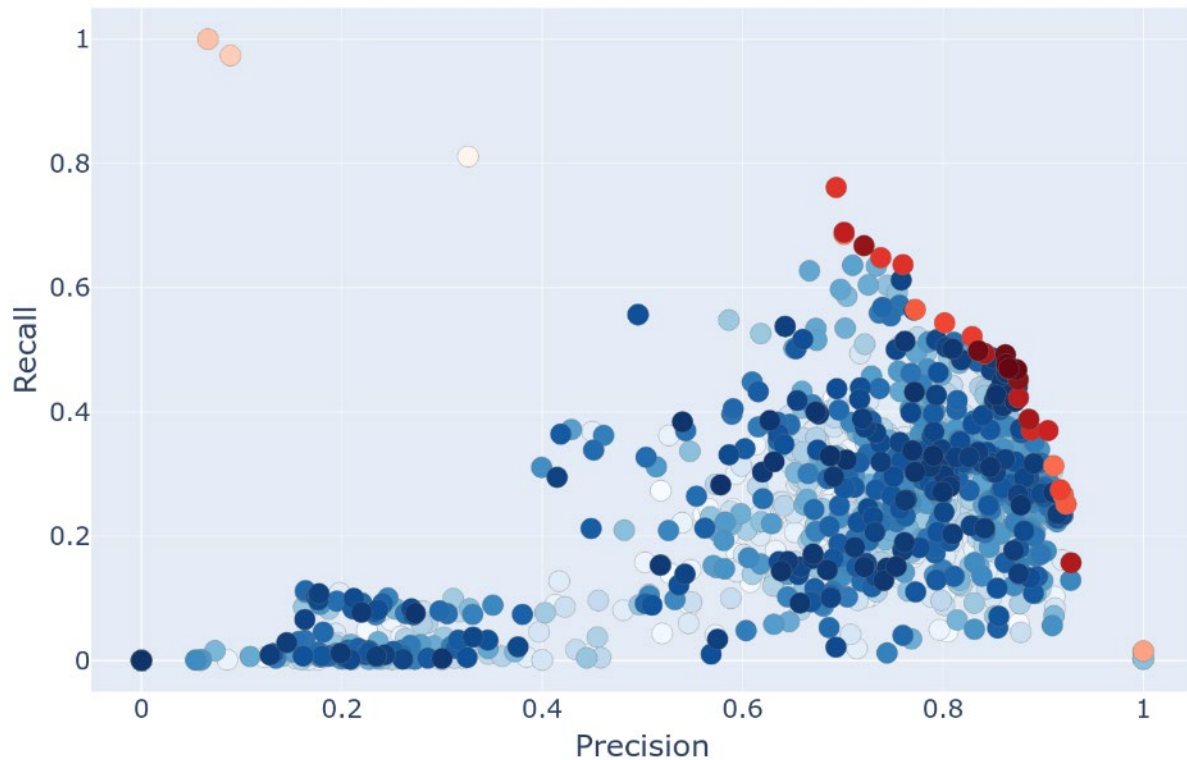


Figure 32: Pareto front of the fitted models. Best trials highlighted in red. Colour saturation indicates the number of trials.

- **TRL achievement level and project SOP**

Because this data analysis software system was used in a simulated deployment under real conditions on recorded data in the lab, the Technology Readiness Level (TRL) declared is 5 for the real-time detection of algal bloom events from Ferrybox data streams. For other types of events TRL 4 is achieved, as the software system is functional, but no conclusions can be drawn concerning its results.

- **Future plans and Recommendations**

Future work will include developing a sampling strategy to control an autosampler on the MS Color Fantasy. It will be based on above event detectors and subject to the following constraints:

- Desired ratio of relevant water samples to missed events
- Number of samples the autosampler can obtain (24 samples)
- Desired maintenance intervals: every 2 days is possible but likely excessive, as samples need to be analysed in the lab

Afterwards, the algorithms can be deployed for tests in the field. Finally, future plans include expansion to other types of events.

To improve event detection results, it is recommended to develop larger data sets, e.g., by covering more years or more locations. Furthermore, having a wider set of reviewers would enable more robust annotations, as the inter-annotator-agreement could be leveraged.

VIII. ETHICAL CONSIDERATIONS

1. DATA PROTECTION

In Task 7.2, raw data and analysis results were exchanged between partners to perform field demonstrations of sensors developed in NAUTILOS. The shared data does not contain classified material, and data was only used if it was shared voluntarily and solely to achieve the project objectives. All processed data that is shared publicly outside the project for project dissemination already follows the procedures defined in D13.2, and in all relations with parties outside the project, the recommended procedures in D13.7 were followed.

2. ENVIRONMENTAL PROTECTION

The sensors were used in controlled environments (ferries) or using drones for close range sensing. In both cases the possibility for a loss of sensors is minimal (or in the case of ferries negligible). In the case sensors used disposable batteries, it was done in accordance with EU regulations, and all battery types were disposed of in designated recycling facilities. Chemicals were used according to safety regulations of each institute involved and no waste was disposed to the sea.

3. HEALTH AND SAFETY

Working onboard ferries was conducted according to safety measures settled by the institutes involved and also following instructions of the ferry companies. All the installations, electrical connections and water connection in ferries were done by qualified and certified personnel. The operations in third party premises (in ferries) was done as agreed with facility owners, following their safety instructions. Specifically, safety equipment (helmets, safety shoes, reflective vest, ear plugs, etc) were used as instructed.

For LIF-LIDAR eye-safety needs to be considered, when deciding in which platform and in which location it is used.

4. PROTECTION OF MARINE LIFE

These sensors rely on non-invasive data collection, allowing them to gather information without disturbing ecosystems. However, high-power lasers could potentially be harmful to animals, particularly those with light-sensitive tissues or specialized visual systems. Nevertheless, LIF-LIDAR is considered an environmentally low-impact and highly beneficial technology when operated responsibly.

5. DUAL USE POTENTIAL

LIDARs are known to be potentially applicable in detecting bioluminescence, and to follow submarines, as submarine movement may mechanically disturb bioluminescent organisms, making them glow and be detectable by LIDARs. The system used here is using different wavebands and is not applicable for such purposes.

Automated samplers may be used to take any time of water samples, also for dual uses. Especially combined with the Ferry Box Stream Data Analysis, these samplers may be driven by any datastreams, triggering samplings at preferred locations.

IX. SUMMARY

This deliverable reports the final demonstration of several sensors developed in NAUTILOS and tested in platforms of opportunity and Ferrybox systems. Demonstrations were done at coastal waters of Norway, the Baltic Sea and the Aegean Sea, using platforms of NIVA, SYKE and HCMR. In addition, DFKI performed Ferrybox stream data analysis to show real-time event detection capabilities.

For downward-looking sensors for ocean platforms and aerial drones, tests were done in coastal Norway using UAVs and ASV. The results were compared with simultaneous Ferrybox measurements. The sensor systems - cameras with UAVs and LIF-LIDAR with ASV - reached a TRL of 7. To improve the systems further, it is advised to test them across varying environmental conditions

The new low-cost infrared temperature sensor was tested onboard a research vessel in the North Aegean, Ionian Sea, and adjacent coastal regions of Greece. Aim of the work was to validate the IR sensor with trusted sensors, like CTDs. In the successful demonstrations the sensor reached TRL level 7. Several points for technical improvements are given and need to be implemented prior to TRL level reaching 9.

The sampler for phytoplankton and other suspended matter was tested in the Ferrybox system in Norway. The sampler was calibrated and validated for Chl-a and eDNA samples during the project. In this report, demonstration of sampler capacities was done using sampling for eDNA, and automated sampler and manually collected/filtered techniques yielded similar DNA concentrations. The study concluded that the TRL level of the sampler is at level 8. Next steps include further verification of the system with long-term deployments and using the system with event detection algorithms developed in NAUTILOS.

The microplastic sampler was successfully demonstrated in coastal Norway, and TRL 7 was reached. TRL levels of Microplastic detector system (sampler + detector + Ferrybox infrastructure) and Microplastic detector were too low (TRL 3-4) to be evaluated in field conditions.

A commercial carbonate system sensor - low-cost pH sensor – with TRL level 9 was tested for oceanographic observations in the Baltic Sea for a period of more than one year. The sensor was compared with high-end spectrophotometric sensor and with commercial buffer solutions. Though sensors differed clearly in their pH values, the difference was rather constant, indicating the issue is with the ability to calibrate low-cost pH sensor appropriately. Drift in calibration was quantified with buffer solutions. Sensor type was found suitable for “weather” level observations (not for “climate” level ones) and for operational oceanographic purposes the system reached TRL level 7. Further tests are planned with additional pH measurements and the observed issues with sensor connectivity will be analysed.

To demonstrate real-time event detection capabilities, using the technologies developed in NAUTILOS and specifically demonstrated in Task 7.2, an annotated data set containing potential algal bloom events was used. In the Task 7.3 the software system was successfully used in a simulated deployment under real conditions on recorded data in the lab, and TRL 5 was reached for the real-time detection of algal bloom events from Ferrybox data streams. Future work with such an approach will include developing a sampling strategy to control an autosampler, e.g. in Ferrybox systems, to take data-driven samples for specific events.

APPENDIX 1: REFERENCES AND RELATED DOCUMENTS

ID	Reference or Related Document	Source or Link/Location
1	Petersen, W. (2014) FerryBox systems: State-of-the-art in Europe and future development. <i>J. Mar. Syst.</i> 14,: 4-12	https://doi.org/10.1016/j.jmarsys.2014.07.003
2	Petersen, W. and Colijn, F. (eds) (2017) FerryBox Whitebook. Brussels, Belgium, EuroGOOS AISBL, 48pp	http://eurogoos.eu/download/publications/EuroGOOS_Ferrybox_whitepaper_2017.pdf
3	Mantovani C., Pearlman J., Simpson P. (Eds.) (2023). JERICO-S3 Deliverable 5.2. Electronic Handbook for Mature Platforms: Mooring - HF Radar - FerryBox – Glider. Version 1.1. (Brest, France: IFREMER for JERICO-S3), 195. JERICO-S3-WP5-D5.2.-310123-V1.1).	https://doi.org/10.25607/OBP-1945
4	Paasche, E.; Ostergren, I. (1980) The annual cycle of plankton diatom growth and silica production in the inner Oslofjord. <i>Limnol. Oceanogr.</i> 25, 481–494.	https://doi.org/10.4319/lo.1980.25.3.0481
5	Pastor, F.; Valiente, J.A.; Khodayar, S. A. (2020) Warming Mediterranean: 38 Years of Increasing Sea Surface Temperature. <i>Remote Sens.</i> 12, 2687.	https://doi.org/10.3390/rs12172687
6	Korres G, Ntoumas M, Potiris M, Petihakis G. (2014) Assimilating Ferry Box data into the Aegean Sea model. <i>J. Mar. Syst.</i> 140, 59-72	https://doi.org/10.1016/j.jmarsys.2014.03.013
7	Delauney L., Lefebvre A. Artigas L. F., Grémare A. King A., Engesmo A., Egge E., Ødegaard Ø. T., Jaccard P., Durand D.(2024). Prototype sensor packages and WASP. Ref. JERICO-S3-WP7-D7.4-300724-V1.1. JERICO S3.	https://doi.org/10.13155/103699
8	Okazaki, R.R., Sutton, A.J., Feely, R.A., Dickson, A.G., Alin, S.R., Sabine, C.L., Bunje, P.M.E. and Virmani, J.I. (2017), Evaluation of marine pH sensors under controlled and natural conditions for the Wendy Schmidt Ocean Health XPRIZE. <i>Limnol. Oceanogr. Methods</i> , 15: 586-600.	https://doi.org/10.1002/lom3.10189
9	Honkanen, M., Aurela, M., Hatakka, J., Haraguchi, L., Kielosto, S., Mäkelä, T., Seppälä, J., Siiriä, S.-M., Stenbäck, K., Tuovinen, J.-P., Ylöstalo, P., and Laakso, L. (2024) Interannual and seasonal variability of the air–sea CO ₂ exchange at Utö in the coastal region	https://doi.org/10.5194/bg-21-4341-2024 , 2024.

	of the Baltic Sea, Biogeosciences, 21, 4341–4359	
10	Müller J.D., Bastkowski F., Sander B., Seitz S., Turner D.R., Dickson A.G. and Rehder G. (2018) Metrology for pH Measurements in Brackish Waters— Part 1: Extending Electrochemical pH Measurements of TRIS Buffers to Salinities 5–20. Front. Mar. Sci. 5:176.	https://doi.org/10.3389/fmars.2018.00176
11	McLaughlin, K., Dickson, A., Weisberg, S. B., Coale, K., Elrod, V., Hunter, C., Johnson, K. S., Kram, S., Kudela, R., Martz, T., Negrey K. (2017) An evaluation of ISFET sensors for coastal pH monitoring applications. Reg. Stud. Mar. Sci., 12, pp. 11-18	https://doi.org/10.1016/j.rsma.2017.02.008